

Obligate biotroph downy mildew consistently induces near-identical protective microbiomes in *Arabidopsis thaliana*

Received: 13 March 2023

Accepted: 13 September 2023

Published online: 16 November 2023

 Check for updates

Pim Goossens^{1,4}, Jelle Spooren^{1,4}, Kim C. M. Baremans¹, Annemiek Andel², Dmitry Lapin^{2,3}, Nakisa Echobardo¹, Corné M. J. Pieterse¹, Guido Van den Ackerveken² & Roeland L. Berendsen¹✉

Hyaloperonospora arabidopsidis (Hpa) is an obligately biotrophic downy mildew that is routinely cultured on *Arabidopsis thaliana* hosts that harbour complex microbiomes. We hypothesized that the culturing procedure proliferates Hpa-associated microbiota (HAM) in addition to the pathogen and exploited this model system to investigate which microorganisms consistently associate with Hpa. Using amplicon sequencing, we found nine bacterial sequence variants that are shared between at least three out of four Hpa cultures in the Netherlands and Germany and comprise 34% of the phyllosphere community of the infected plants. Whole-genome sequencing showed that representative HAM bacterial isolates from these distinct Hpa cultures are isogenic and that an additional seven published Hpa metagenomes contain numerous sequences of the HAM. Although we showed that HAM benefit from Hpa infection, HAM negatively affect Hpa spore formation. Moreover, we show that pathogen-infected plants can selectively recruit HAM to both their roots and shoots and form a soil-borne infection-associated microbiome that helps resist the pathogen. Understanding the mechanisms by which infection-associated microbiomes are formed might enable breeding of crop varieties that select for protective microbiomes.

Downy mildews are plant-pathogenic oomycetes that cause major damage to a wide variety of plant species¹. These pathogens have an obligate biotrophic lifestyle and are host specific². Plants have an innate immune system that relies on the recognition of the pathogen using cell-surface pattern recognition receptors and *R* genes that encode intracellular nucleotide-binding leucine-rich repeat receptors³. In the model plant *Arabidopsis thaliana* (hereafter *Arabidopsis*), resistance to its cognate downy mildew *Hyaloperonospora arabidopsidis* (Hpa) is based on the recognition of pathogen-produced immunomodulatory

effector proteins by nucleotide-binding leucine-rich repeat receptors of the RESISTANT TO PERONOSPORA PARASITICA (RPP) family^{4,5}.

Plants accommodate diverse microbiomes in virtually all tissues. The aboveground plant parts, known as the phyllosphere, host microbial communities that are less abundant and diverse than those in the rhizosphere⁶, the part of the soil that is directly influenced by plant roots⁷. Microbiomes in the rhizosphere and phyllosphere can protect plants from pathogens^{8,9}. Beneficial microorganisms can inhibit pathogen growth by direct antagonism or by increasing the competence of

¹Plant–Microbe Interactions, Institute of Environmental Biology, Department of Biology, Science4Life, Utrecht University, Utrecht, the Netherlands.

²Translational Plant Biology, Institute of Environmental Biology, Department of Biology, Science4Life, Utrecht University, Utrecht, the Netherlands.

³Plant–Microbe Interactions, Max Planck Institute for Plant Breeding Research, Cologne, Germany. ⁴These authors contributed equally: Pim Goossens, Jelle Spooren. ✉ e-mail: r.l.berendsen@uu.nl

the plant immune system^{10,11}. It has been proposed that the microbiome functions as an extension of the plant immune system, providing an additional layer of defence against pathogen attack¹².

Leaf infection of *Arabidopsis* by Hpa results in the recruitment of a community of protective bacteria in the rhizosphere. A synthetic three-member consortium consisting of a *Xanthomonas* sp., a *Stenotrophomonas* sp. and a *Microbacterium* sp. reduced susceptibility to Hpa and promoted plant growth¹³. Plants grown in soil that was previously used to grow Hpa-infected plants were more resistant to Hpa than plants grown in soil used to grow uninfected plants¹³. Infections by other leaf bacterial^{14,15} and fungal¹⁶ pathogens, or a root-feeding insect herbivore¹⁷, also showed that plants can recruit microbiota upon pathogen attack and create a persistent protective soil microbiome, called a soil-borne legacy^{18,19}. Recently, we reported that mutant plants impaired in defence signalling via the plant hormone salicylic acid are not protected by an Hpa-induced soil-borne legacy, suggesting that the legacy may enable defence by affecting plant salicylic-acid-dependent immunity²⁰. Outside of the lab, the pathogen-induced build-up of beneficial microorganisms in agricultural fields is proposed to result in disease-suppressive soils^{21,22}.

Disease-associated microbiomes are probably shaped by a combination of plant- and pathogen-driven selective pressures. Hpa cultures are maintained at research institutes by weekly washing of spores from diseased plants then transmitting them to healthy plants²³. Different isolates of Hpa, with distinct effector repertoires, are cultured on specific *Arabidopsis* accessions that lack the corresponding *RPP* gene(s)^{5,23}. Therefore, Hpa cultures represent systems in which distinct pathogen isolates have, since their isolation in the early 1990s²⁴, completed many life cycles on their host in association with a microbiome. We hypothesized that different Hpa cultures represent an excellent system to investigate infection-induced microbiome recruitment.

Here we investigated phyllosphere microbiome compositions of *Arabidopsis* plants after infection with different Hpa isolates and evaluated how pathogen-induced microbiomes function in plant defence.

Phyllosphere microbiota are passaged with but not on Hpa spores

First, we characterized phyllosphere microbiomes of *Arabidopsis* plants that were infected with Hpa isolate Noco2 (ref. 25). Infection was established in two different ways. Spore suspensions were prepared by washing Noco2-infected leaves with water and spraying the wash-off, which contains the spores, onto susceptible 10-day-old Col-0 plants (water inoculation). This is the routine method by which Hpa cultures are passaged weekly in most research institutes. In addition, Col-0 plants were inoculated by placing a pot containing plants below a pot of Hpa-infected plants and dispersing spores from the infected plants using a compressed air pulse (wind inoculation). Untreated Col-0 plants were controls. Seven days post-inoculation (dpi), we quantified Hpa by quantitative PCR and processed samples for microbiome analysis using 16S ribosomal RNA gene (16S; bacterial) and internal transcribed spacer region 2 (ITS2; fungal) amplicon sequencing.

Hpa was detected in the leaves of water-inoculated and wind-inoculated plants (Extended Data Fig. 1a). However, the phyllosphere microbiomes of the water-infected plants differed significantly (false-discovery-rate (FDR)-adjusted $P < 0.001$) from those of untreated control plants in permutational multivariate analysis of variance (PERMANOVA; $R^2 = 0.36$). This difference was also reflected by a principal coordinate analysis (PCoA) ordination plot based on Bray–Curtis dissimilarities of the communities (Extended Data Fig. 1b). Wind inoculation did not significantly change the composition of the phyllosphere community (PERMANOVA; $R^2 = 0.1$, $P = 0.24$). We observed 26 amplicon sequence variants (ASVs) that were significantly enriched ($P < 0.05$, DESeq2 (ref. 26), \log_2 fold change > 1) in water-inoculated samples compared with untreated controls, whereas only a single, different ASV

was enriched after wind inoculation (Supplementary Table 1). These data led us to propose that in water inoculation, some phyllosphere bacteria are passaged with the Hpa spores, but that these bacteria are not present on wind-inoculated spores. Neither inoculation treatment significantly affected phyllosphere fungal community composition (Extended Data Fig. 1c), so our subsequent experiments assessed only bacterial community data.

Hpa cultures contain similar Hpa-associated microbiomes

Next, we evaluated whether similar phyllosphere communities were induced by different Hpa lineages. We inoculated plants with either Hpa Noco2 (ref. 25) or Hpa Cala2 (ref. 24). These isolates have been separately cultured in our research institute for the past 24 years. Ten-day-old plants of the *Arabidopsis* accessions C24 (ref. 27), Col-0, Ler and Pro-0 (ref. 28) were inoculated with Noco2, Cala2, a mix of both isolates or sterile water (mock). These accessions were selected because they are either susceptible or resistant to Noco2 and/or Cala2 (Fig. 1a and Extended Data Fig. 2). Seven dpi, when Hpa had started sporulating on the susceptible accessions, we analysed bacterial phyllosphere community compositions. Amplicon sequencing of the 16S ribosomal RNA (rRNA) genes showed that the composition of the bacterial phyllosphere community was affected by Hpa inoculation (Fig. 1b). Inoculation with either Noco2 or Cala2 spore suspensions resulted in phyllosphere communities that were significantly different from each other ($P < 0.05$ in PERMANOVA; Supplementary Table 2). Mix-inoculated samples were intermediate between Noco2- and Cala2-inoculated samples (Fig. 1b). Plant genotype had a small but significant effect, but the phyllosphere bacterial community changed following inoculation with Hpa regardless of the plant accession's susceptibility (Fig. 1b and Supplementary Table 4). We conclude that Hpa spores washed from an infected leaf are passaged together with a bacterial community.

In these samples, we identified 161 bacterial 16S ASVs that significantly changed in abundance ($P < 0.05$, DESeq2 (ref. 26)) as a result of inoculation with at least 1 Hpa isolate. Among them, 17 ASVs were enriched on both Noco2- and Cala2-inoculated plants (Fig. 1c). These 17 ASVs comprise 45% of the bacterial phyllosphere communities on the Hpa-inoculated plants (Fig. 1c,e,f and Supplementary Fig. 1). Conversely, 53 ASVs were significantly depleted on all Hpa-inoculated plants, but constituted 47% of the bacterial communities on mock-treated plants (Fig. 1d,e and Supplementary Fig. 1). Therefore, although inoculation with two different Hpa isolates leads to a distinct phyllosphere microbiome, these microbiomes are dominated by bacteria with identical ASVs (Fig. 1f).

The Noco2 and Cala2 cultures in Utrecht have been maintained separately since 1999. Cross-contamination has always been monitored using plant accessions that are resistant to the Hpa isolate being cultured, but susceptible to other Hpa isolates. It is therefore remarkable to find that the same 17 ASVs form such a large part of the bacterial microbiome of both the Noco2 and the Cala2 cultures in Utrecht.

To test whether the enrichment for these distinct Hpa-associated microbiota is a local peculiarity or more broadly applicable to *Arabidopsis* downy mildews, we collected Col-0 and Ler samples infected with Noco2 or Cala2, or inoculated with water (mock), at a different location, the Max Planck Institute for Plant Breeding Research (Cologne, Germany), which have independently maintained the same isolates for many years. Consistent with observations made in Utrecht, Hpa inoculation with either Noco2 or Cala2 significantly altered the bacterial phyllosphere community (Fig. 2a). We found 57 ASVs enriched in at least 2 Hpa cultures from either or both geographic locations (hereafter frequently Hpa-enriched ASVs; pink to red in Fig. 2b–d) including 4 ASVs enriched in all 4 Hpa cultures across both locations (hereafter Hpa-core ASVs; Fig. 2e; red in Fig. 2). These 57 frequently

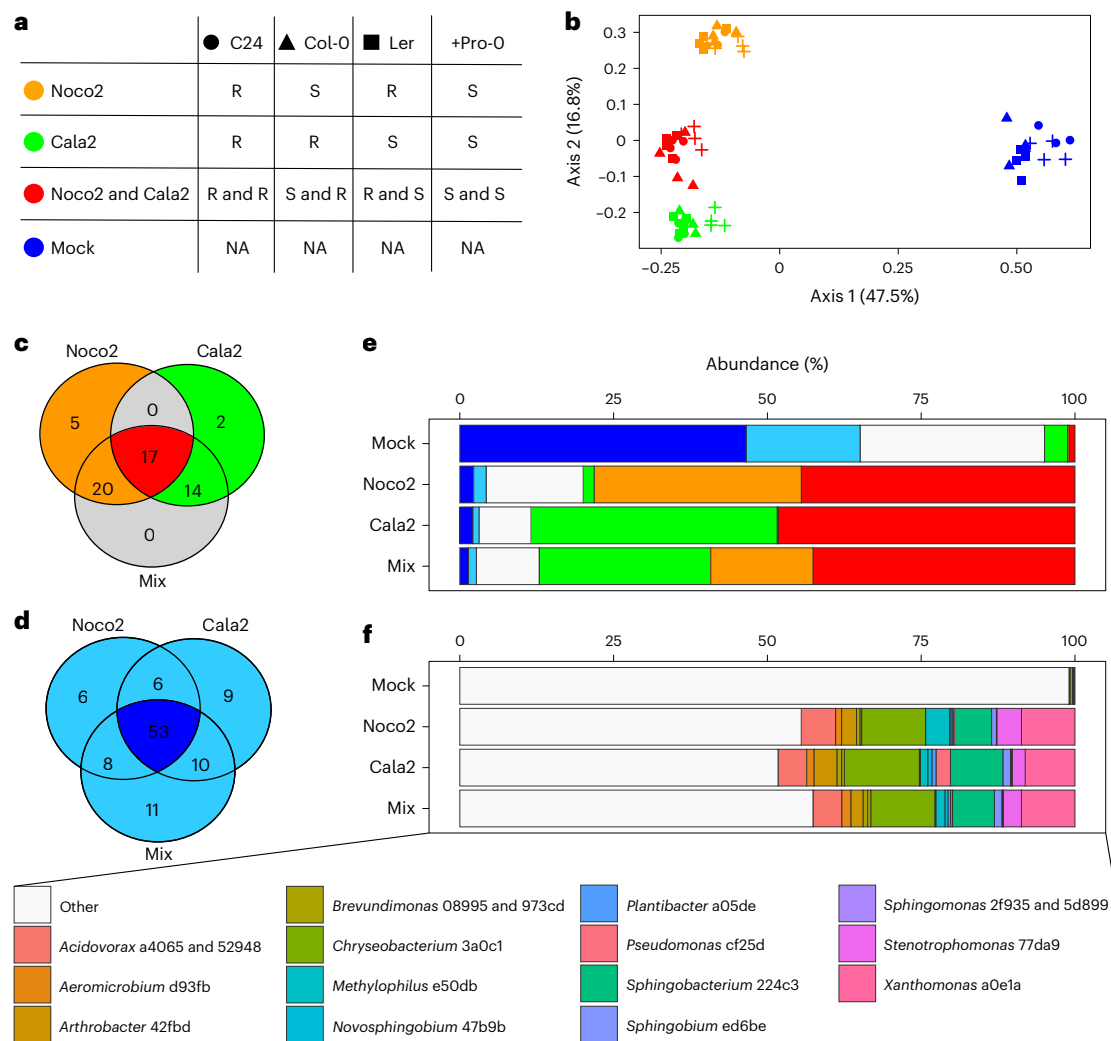


Fig. 1 | Distinct Hpa cultures are enriched for identical ASVs that dominate the phyllosphere bacterial communities. **a**, Overview of the susceptibility of each Arabidopsis accession to Noco2 and Cala2. S, susceptible. R, resistant. NA, not applicable. Hpa isolate colour codes and Arabidopsis accession shapes also function as a guide to colours and shapes in **b**. **b**, PCoA ordination plot based on Bray–Curtis dissimilarities of the bacterial phyllosphere communities of Arabidopsis accessions Col-0, C24, Ler or Pro-0 following inoculation with sterile water (mock), spore suspensions of Hpa isolates Noco2 or Cala2, or a mix of both isolates ($N = 4$ distinct biological replicates per treatment; for C24, $N = 3-4$). **c,d**, Venn diagrams of significantly enriched (**c**) and significantly depleted (**d**)

ASVs in Hpa-inoculated plants compared with those of mock-inoculated plants (FDR-corrected $P < 0.05$, DESeq2 (Wald test)). **e**, Stacked chart of the relative abundance of the 17 ASVs that were enriched in all Hpa-inoculated groups (red), those that were enriched in either Noco2-inoculated (orange) or Cala2-inoculated (green) plants, the 53 ASVs that were depleted in all Hpa-inoculated groups (dark blue) or ASVs that were depleted in two or fewer Hpa-inoculated groups (light blue), and all other ASVs in the data (white) in each inoculation group. **f**, Stacked chart highlighting the abundances and taxonomies of the ASVs that were significantly enriched in Noco2- and Cala2-inoculated plants.

Hpa-enriched ASVs occupy up to 75% of the phyllosphere bacterial communities of Hpa-inoculated plants at both locations and are low abundant or undetected in mock-treated samples (Fig. 2c).

The 57 frequently Hpa-enriched ASVs corresponded to taxonomically diverse bacteria representing 9 bacterial classes and 38 genera (Fig. 2d). The Hpa-core ASV a0e1a, annotated as a *Xanthomonas* sp., was consistently highly abundant in the four Hpa cultures that were investigated and comprised between 5% and 10% of the bacterial phyllosphere population in all inoculated samples (Fig. 2e). The other three Hpa-core ASVs were consistently enriched but less abundant than *Xanthomonas* a0e1a (Fig. 2e). The nine ASVs that occurred in at least three out of four Hpa isolates formed 34% of the phyllosphere community on average in all inoculated samples.

Our results show that repeated passaging of Hpa and associated microorganisms during Hpa maintenance resulted in the enrichment of a similar small set of taxonomically diverse bacterial ASVs.

Separate Hpa cultures contain isogenic Hpa-associated microbiota

To characterize the Hpa-associated microbiota (HAM), we generated a collection of 702 bacterial isolates from Arabidopsis leaves that were infected by Noco2 or Cala2 in Utrecht or Cologne, and characterized individual isolates by sequencing 16S rRNA amplicons. Then, we sequenced the whole genome of 31 isolates, selected to represent 8 HAM ASVs including the 4 Hpa-core ASVs and originating from separate cultures. The 16S rRNA amplicons of the 31 isolates matched either *Xanthomonas* HAM ASV a0e1a, *Acidovorax* HAM ASV a4065, *Sphingobium* HAM ASV ed6be, *Arthrobacter* HAM ASV 42fbd, *Aeromicrobium* HAM ASV d93fb, *Methylobacterium* HAM ASV 15da8, *Microbacterium* HAM ASV f0c76 or *Rhizobium* HAM ASV 2569b. Genomes of isolates that matched with the same ASV were mostly isogenic (average nucleotide identity (ANI) $> 99.99\%$)²⁹, even when the isolates were obtained from distinct and geographically separated Hpa cultures (Supplementary

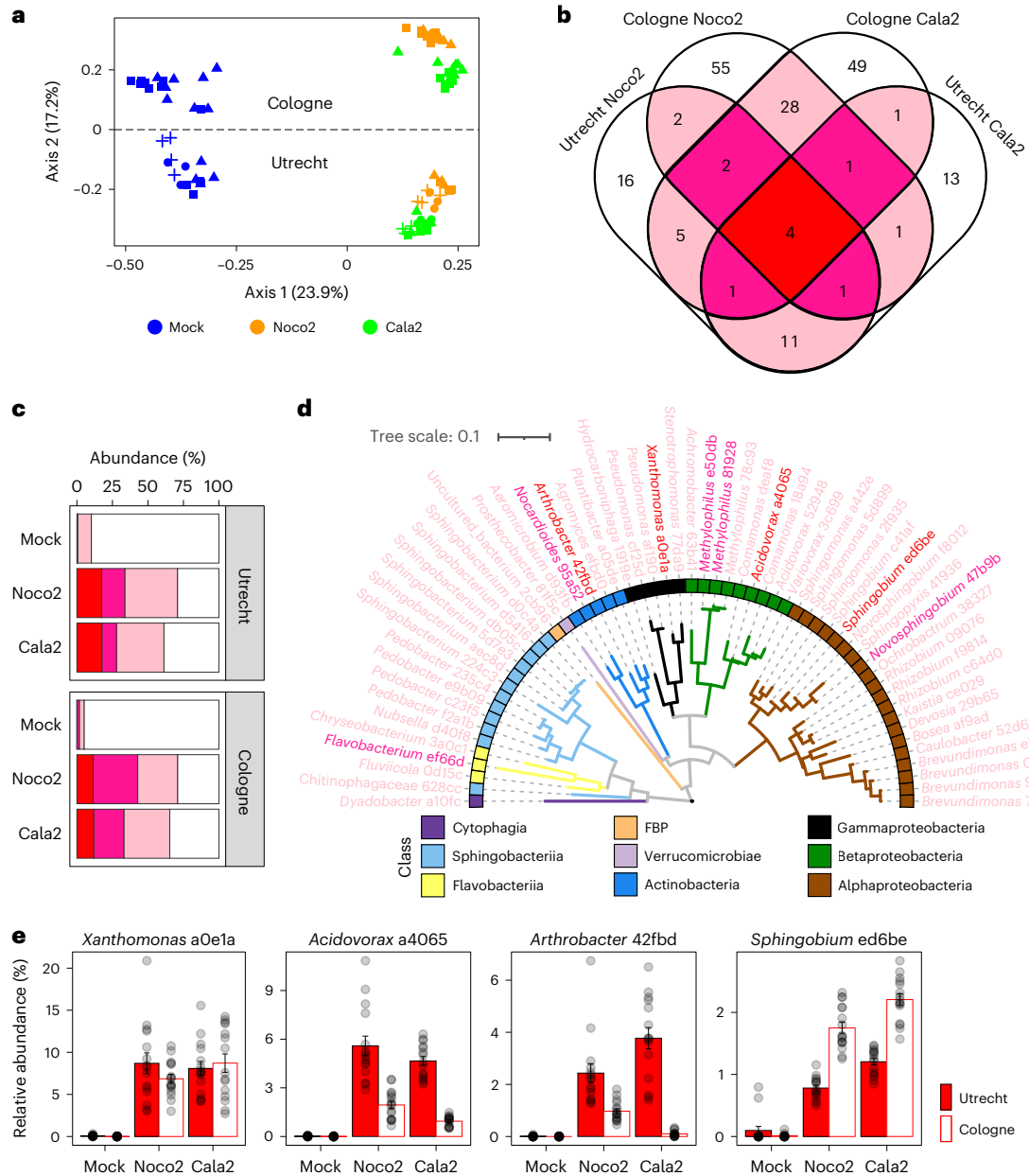


Fig. 2 | Hpa cultures from Utrecht and Cologne are enriched for identical ASVs. **a**, PCoA ordination plot based on Bray–Curtis dissimilarities of the bacterial phyllosphere communities of Arabidopsis accession Col-0 (triangles), C24 (circles), Ler (squares) or Pro-0 (plus symbols) following inoculation with sterile water or a spore suspension of Hpa isolate Noco2 or Cala2 cultured and maintained at Utrecht ($N = 4$ per genotype) and Cologne ($N = 8$ per genotype). **b**, Venn diagram of frequently Hpa-enriched ASVs that are significantly enriched in two (light pink), three (dark pink) or four (red) of the Hpa cultures. **c**, Stacked chart with the cumulative relative abundance of the frequently Hpa-enriched ASVs that are enriched in two (light pink), three (dark pink) or four (red) Hpa

cultures. **d**, Dendrogram based on MAFFT alignment of frequently Hpa-enriched ASVs that were significantly enriched in at least two out of four Hpa cultures. Colours of taxonomy labels indicate significant enrichment in two (light pink), three (dark pink) or four (red) Hpa cultures. Colours as indicated in the legend below the figure indicate ASV class. FBP, Faba Bean Phylo group. The tree scale represents the proportion of non-identical nucleotides between genomes ranging from 0 to 1. **e**, Bar charts of mean abundances of the four ASVs that were consistently enriched in the Noco2 and Cala2 cultures at Utrecht and Cologne. Error bars represent standard error. $N = 15$ or 16 biologically independent samples.

Fig. 2). Similarly, alignment coverages between these genomes were between 95% and 100% with an average coverage of 99.8% (Supplementary Fig. 3). Only the two *Microbacterium* isolates (*Microbacterium* f0c76-1 and *Microbacterium* f0c76-2) that represented HAM ASV f0c76 were found not to be isogenic (ANI = 88.5%; Supplementary Fig. 2). Both *Microbacterium* isolates were used in subsequent analyses.

We used these nine distinct HAM bacterial genomes to investigate the presence of HAM bacteria in seven additional independent Hpa cultures. To this end, we made use of raw sequencing data underlying seven publicly available Hpa genomes that had all been produced

from spores of Hpa-infected plants because these raw sequencing data represent Hpa metagenomes of Hpa and its microbiome. These seven metagenomes were obtained either by Sanger sequencing of selected bacterial artificial chromosome (BAC) clones derived from Hpa isolate Emoy2 (ref. 30) or Illumina sequencing of the Hpa isolates Emoy2, Hind2, Cala2, Emco5, Emwa1 and Maks9 (ref. 31). They were all originally isolated in the United Kingdom and were maintained by regular transfer of Hpa spores from infected plants to a new batch of uninfected plants in laboratories located in East Malling (now Warwick University)³⁰ and Norwich (Sainsbury Laboratory)³¹.

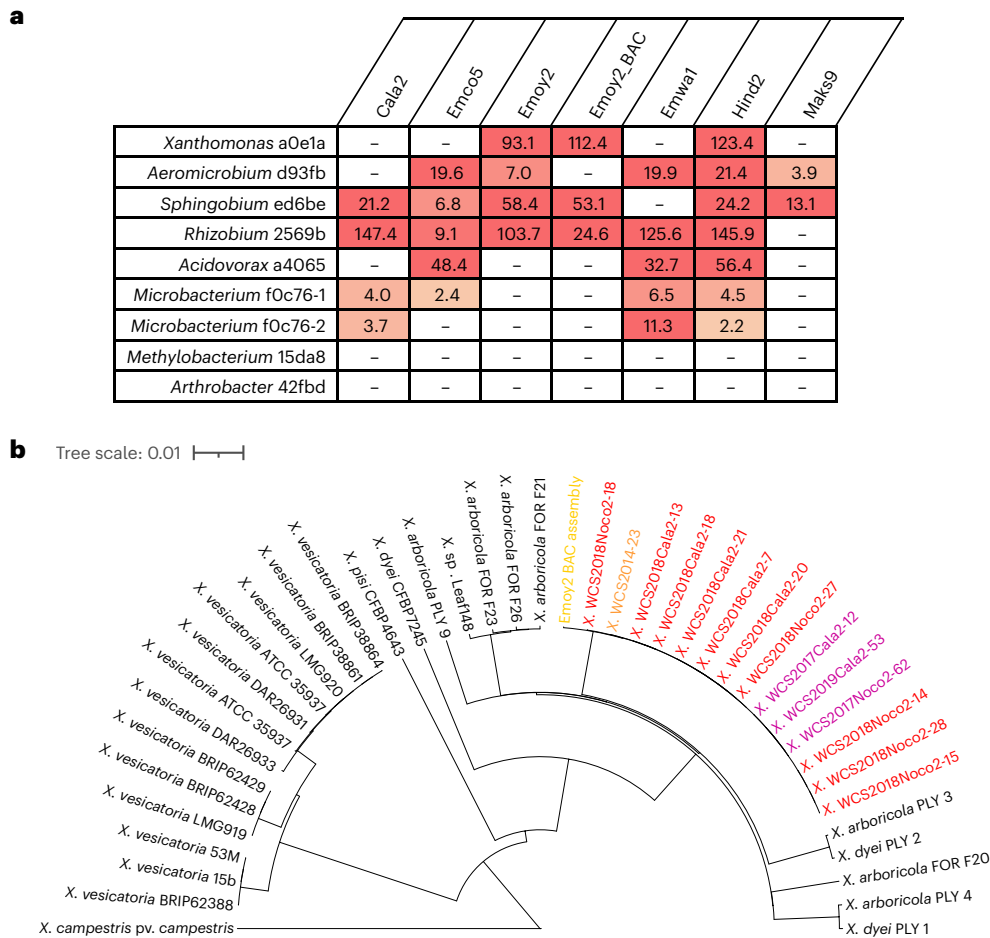


Fig. 3 | Isogenic HAM bacterial genomes are present in metagenomes of geographically separated Hpa cultures. **a**, Heat map indicating the presence of specific HAM bacterial genomes in publicly available Hpa metagenomes. The numbers indicate signal-to-noise ratios, in which signal represents the number of reads that were assigned to a specific genome, and background noise was calculated as the total number of reads that were assigned to all genomes within a specific genus, divided by the number of genomes within that genus. Genomes with a signal-to-noise ratio below 2 were considered undetected (-). **b**, Dendrogram based on unweighted pair group method with arithmetic

mean (UPGMA) hierarchical clustering of a (1 - ANI) distance matrix for all *Xanthomonas a0e1a* isolates that were sequenced (red indicates isolates from Utrecht; purple indicates isolates from Cologne), *Xanthomonas* sp. WCS2014-23 (indicated in orange), a *Xanthomonas* sp. genome assembly using Sanger reads from an Emoy2-derived BAC library (indicated in yellow), the 25 most-related *Xanthomonas* genomes in the refseq database and *Xanthomonas campestris* pv. *campestris* as outgroup. The tree scale represents branch length corresponding to the proportion of non-identical nucleotides between genomes.

Reads from the Hpa metagenomes were pseudo-aligned³² to a genome index containing the 9 distinct HAM bacterial genomes and all available unique genomes (<98% ANI) of the 8 corresponding genera (in total 1,128 genomes; Supplementary Table 5 and Supplementary Figs. 4–11). In this way, the majority of bacterial genomes within the index were assigned only a few reads from every Hpa metagenome (considered background noise). By contrast, we generally observed a few genomes per genus that were assigned far more reads than the background noise (Supplementary Figs. 4–12). Using this method, we detected the presence of seven out of nine HAM bacterial genomes in multiple of the seven Hpa metagenomes (Fig. 3a and Supplementary Figs. 4–11). Only the *Arthrobacter* and *Methylobacterium* HAM genomes were not detected in any of the Hpa metagenomes. In each of the investigated metagenomes, at least two of these seven bacteria were detected and all seven HAM bacteria were detected in the metagenome of the Hpa Hind2 isolate.

The Emoy2 metagenome, which was derived from a BAC library³⁰ and published in 2010, consisted of longer high-quality reads than the Illumina-based metagenomes³¹, and a large number of BAC-derived reads were assigned to the *Xanthomonas a0e1a* genome (Supplementary Fig. 12). We were able to partially reassemble the *Xanthomonas*

BAC clones from which these reads originated. This resulted in the assembly of seven contigs ranging from 9,844 bp to 62,269 bp, with a total length of approximately 233 kb, and these contigs shared an ANI of 99.97% with the *Xanthomonas a0e1a* genomes from the Utrecht and Cologne Hpa isolates from this study (Fig. 3b and Supplementary Fig. 13). This confirms that the Hpa metagenome reads assigned to the *Xanthomonas a0e1a* genome are indeed derived from a bacterium that is isogenic to *Xanthomonas a0e1a* genomes isolated in this study. Intriguingly, the *Xanthomonas a0e1a* isolates were also isogenic to *Xanthomonas* sp. WCS2014-23 (Fig. 3b), previously isolated in our lab as part of a plant-protective consortium of microorganisms from the roots of downy-mildew-infected plants¹³.

Together, these results show that although none of the HAM bacteria are obligately associated with Hpa, different combinations of these HAM bacteria were always present in each of the 11 distinct Hpa cultures tested. Although the HAM comprises bacteria of diverse taxonomy, isogenic representatives of the HAM taxa are enriched in strictly separated Hpa cultures maintained in British, Dutch and German research institutes.

We propose that different cultures of Hpa isolates have independently acquired similar consortia of isogenic HAM bacteria, and

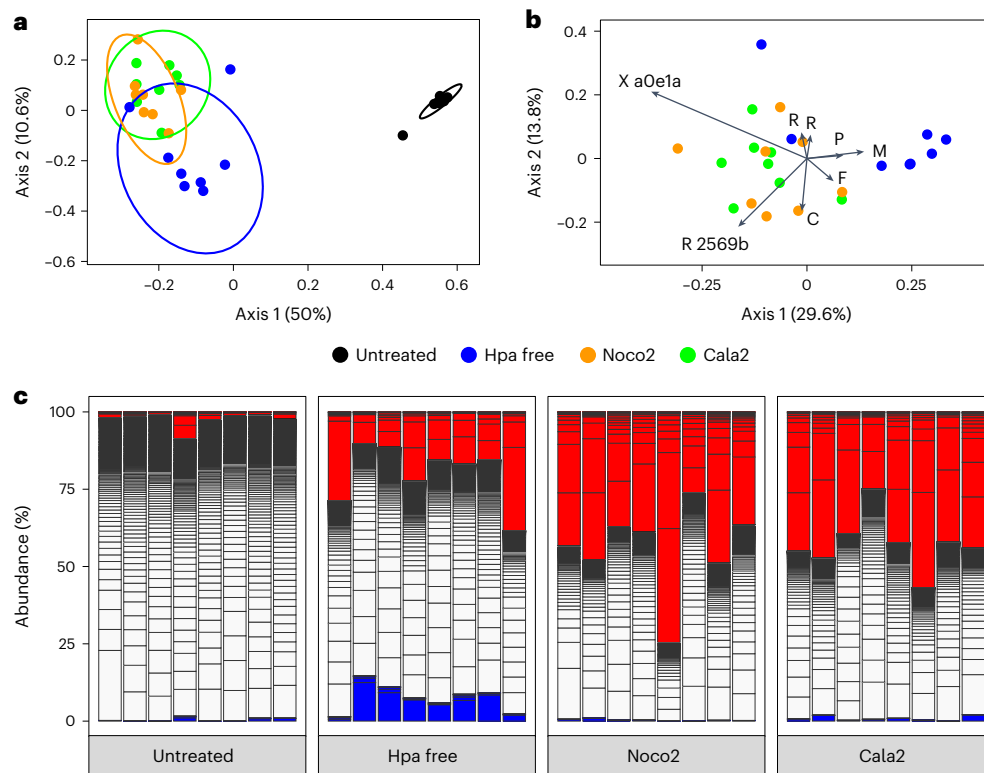


Fig. 4 | HAM ASV abundances diminish in the absence of Hpa. a, PCoA ordination plot based on Bray–Curtis dissimilarities of phyllosphere bacterial communities following nine HAM passages over *Arabidopsis* Ler/*rpp5* plants in the presence of Hpa isolate Noco2 (lineage 1, orange symbols) or Cala2 (lineage 2, green symbols), or in the absence of Hpa (lineage 3, blue symbols). Black symbols show phyllosphere microbiomes of plants that were left untreated (lineage 4). Ellipses represent multivariate *t*-distributions with a 95% confidence level. $N = 8$ distinct biological replicates per lineage that were passaged separately for the duration of the experiment. **b**, PCoA ordination biplot similar to **a**, without untreated samples. Arrows indicate the relative contribution of individual ASVs

to the first two principal coordinate axes. Shown are the top five contributors for each axis (eight ASVs as two ASVs were top contributors to both axes). X aOe1a, *Xanthomonas* ASV aOe1a; R 2569b, *Rhizobium* ASV 2569; P, *Pseudomonas*; M, *Methylophilus*; F, *Flavobacterium*; C, *Chryseobacterium*. **c**, Stacked bar chart with the relative abundances of the ASVs that are significantly enriched (red), depleted (blue) or unaffected (white) in Noco2- (lineage 1) and Cala2-infected (lineage 2) samples compared with those of Hpa-free cultures (lineage 3). Each bar represents the ninth passage of an independent lineage of passages or an untreated sample (lineage 4) grown at the same time.

hypothesize that Hpa-infected leaves selectively recruit and select specific bacteria.

HAMs are selected by Hpa infection

We next investigated whether HAM enrichment on infected leaves is driven by the interaction with Hpa or by HAM members outcompeting other microorganisms in the *Arabidopsis* phyllosphere. To investigate HAM development in the absence of Hpa, we made use of the gene *RPP5*, which provides resistance to Noco2 in wild-type Ler plants and in transgenic Col-0 *RPP5* plants²⁵, rendering the latter resistant to both Noco2 and Cala2. As Noco2 and Cala2 have distinct HAMs (Fig. 1), spore suspensions of these two cultures were mixed in equal proportions to make an Hpa inoculant with a uniform HAM (uHAM). This uniform inoculant was used to inoculate three lineages of plants: wild-type Col-0 (resistant to Cala2, so this lineage harbours only Noco2 spores and microbiota from uHAM), Ler plants (resistant to Noco2, so this lineage harbours only Cala2 spores and microbiota from uHAM) and transgenic Col-0 *RPP5* plants (resistant to both isolates, so this lineage contains only the microbiota from uHAM).

One week after inoculation, wash-offs from leaves of these three lineages of plants were prepared and used to inoculate Ler *rpp5* plants³³, which are susceptible to both Noco2 and Cala2 (Extended Data Fig. 3). Subsequently, the phyllosphere wash-offs from lineage 1 (Noco2 plus uHAM), lineage 2 (Cala2 plus uHAM) and lineage 3 (only uHAM) were passaged every week to a new population of susceptible Ler *rpp5* plants for a total of nine consecutive passages, such that eight independent

phyllosphere cultures were passaged per lineage. Lineage 3 Ler *rpp5* plants did not develop Hpa infections, indicating that the experiment remained free from cross-contamination. Untreated Ler *rpp5* plants were included as an additional negative control (Extended Data Fig. 3). We analysed the bacterial phyllosphere microbiomes from all three lineages and untreated plants at the end of the first, fifth and ninth passage on Ler *rpp5* by 16S amplicon sequencing.

At each of these timepoints, phyllosphere microbiome communities of untreated controls were clearly distinct from the inoculated phyllosphere samples of lineages 1–3 (Extended Data Fig. 4, Fig. 4a and Supplementary Table 6; $P < 0.05$ in PERMANOVA), suggesting that the uHAM persists to a certain extent even in the absence of Hpa. However, while uHAM microbiomes associated with either Noco2 or Cala2 were similar, they differed significantly from the Hpa-depleted uHAM communities (Extended Data Fig. 4 and Supplementary Tables 6 and 7). These Hpa effects were detectable after the first Ler *rpp5* passage but were more evident after passages 5 and 9 (Supplementary Table 7 and Extended Data Fig. 4). This shows that Hpa infection significantly affects phyllosphere microbiome composition.

Next, we focused specifically on passage 9 to further study the effect of the removal of Hpa from its associated microbial community (Fig. 4a). A PCoA biplot (Fig. 4b) shows that the previously observed *Xanthomonas* ASV aOe1a is the strongest contributor to the separation of the Noco2- and Cala2-infected plants from the Hpa-free cultures, highlighting that this bacterium is most strongly associated with downy mildew infection. Differential abundance testing revealed 18 ASVs that

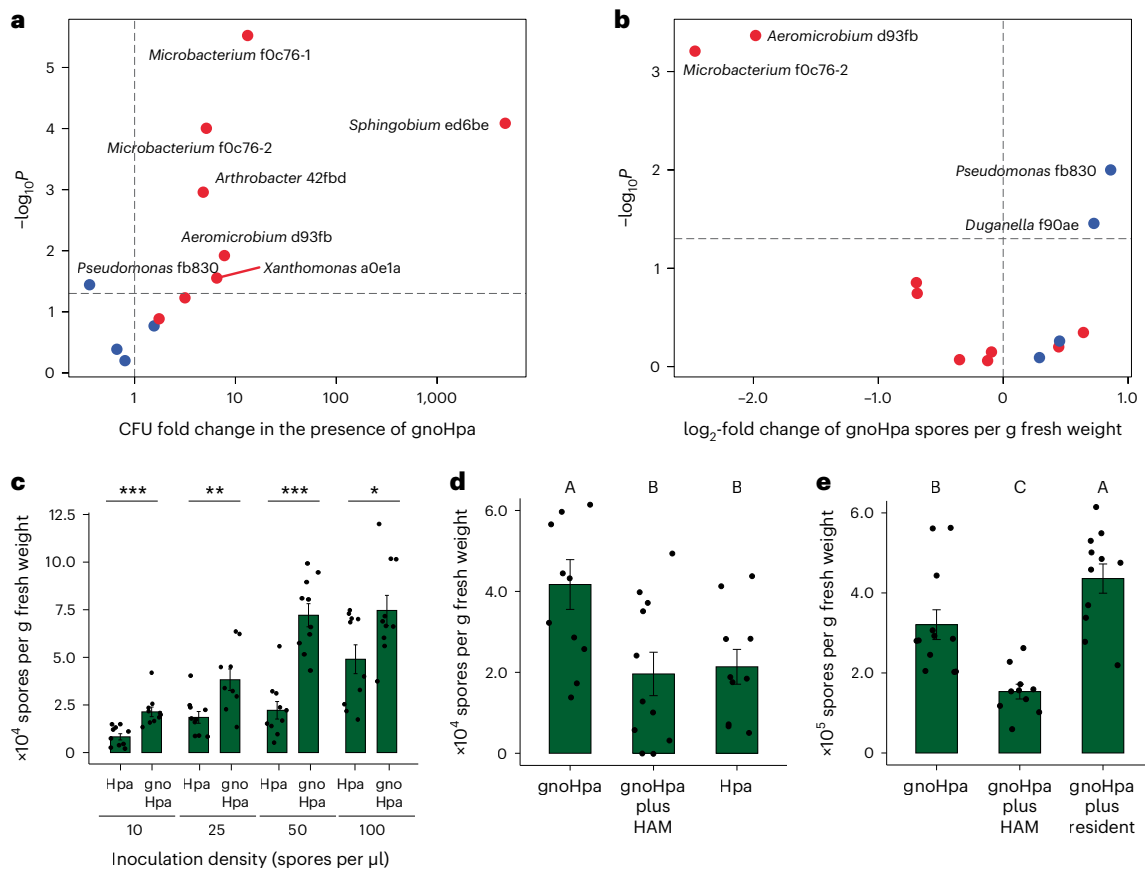


Fig. 5 | HAM bacteria benefit from the presence of Hpa in a gnotobiotic system and can reduce disease. **a**, Fold change in bacterial abundance of HAM isolates 7 days after inoculation of each isolate separately on axenic plants with or without gnoHpa spores. **b**, Fold change in Hpa spore production in the presence or absence of single bacterial isolates. Each dot in the scatter plots represents the average fold change on treated plants compared with that in control plants. In **a** and **b**, P values plotted on the y axis were calculated with Wilcoxon test (two tailed). Red dots denote HAM bacterial isolates that represent *Xanthomonas* HAM ASV a0e1a, *Acidovorax* HAM ASV a4065, *Sphingobium* HAM ASV ed6be, *Arthrobacter* HAM ASV 42fbd, *Aeromicrobium* HAM ASV d93fb, *Methylobacterium* HAM ASV 15da8 and two isolates representing *Microbacterium* HAM ASV f0c76. Blue dots represent phyllosphere-resident isolates (Supplementary Table 9). The vertical dashed lines separate negative (left) and positive (right) effects on bacterial abundance (**a**) and Hpa spore production (**b**). The horizontal line indicates the significance threshold ($P = 0.05$) above which significant

differences are shown. Isolate names are only included in the plots if they are above this significance threshold. **c**, Bar graph of Hpa and gnoHpa spore production 1 week post-inoculation with different inoculum spore densities. The bars show the mean of nine to ten biologically independent samples; error bars indicate standard error. Asterisks indicate significance in one-sided Student's t -test: (left to right) $***P = 2.0 \times 10^{-4}$; $**P = 0.0029$; $***P = 1.8 \times 10^{-6}$; $*P = 0.016$. **d**, Bar graph of Hpa spore production following inoculation of 14-day-old Arabidopsis plants with gnoHpa spores, gnoHpa amended with HAM filtrate or regular Hpa spore suspensions. **e**, Bar graph of Hpa spore production following inoculation of 14-day-old Arabidopsis plants with gnoHpa spores, gnoHpa amended with HAM filtrate or gnoHpa amended with the microbiome filtrate of healthy plants (resident). Bars in **d** and **e** show the mean of 10–12 biologically independent samples. Error bars depict the standard error. Capital letters show significant differences (analysis of variance with Tukey's post hoc test).

were enriched in the phyllosphere of infected plants compared with Hpa-free inoculated plants (Supplementary Table 8). Whereas the 18 enriched ASVs occupy on average 44% of the total phyllosphere communities of Hpa-infected plants, they represent approximately 20% of the communities in Hpa-free cultures, while they are largely absent in untreated control plants (Fig. 4c). Strikingly, the Hpa-infected plant phyllospheres of passage 9 were dominated by *Xanthomonas* ASV a0e1a, whereas, in the Hpa-free phyllospheres, *Xanthomonas* ASV a0e1a abundance was diminished (Supplementary Fig. 14 and Table 8). Thus, the presence of Hpa benefits specific HAM bacteria in the phyllosphere, among which are, most prominently, *Xanthomonas* ASV a0e1a.

HAM bacteria suppress Hpa sporulation

We then wondered whether the abundance of individual HAM species on leaves would increase as a result of infection with Hpa. To test this, we generated a gnotobiotic culture of Hpa isolate Noco2 (henceforth gnoHpa). This culture was created by carefully inoculating healthy

Arabidopsis seedlings, grown axenically on agar-solidified medium, by touching the seedlings with the sporangiophores of Hpa extending from a detached and infected Arabidopsis leaf. After three subsequent careful passages of Hpa in this gnotobiotic system, leaf wash-offs from this in vitro Arabidopsis–Hpa culture were plated on different cultivation media. No microbial growth was observed, indicating that the gnoHpa culture was cleared from its HAM and underlining that the Hpa spores do not carry HAM bacteria.

Next, gnoHpa spores were co-inoculated with the individual HAM isolates (Fig. 3 and Supplementary Table 9) or with four individual isolates that represent ASVs that were not enriched on Hpa-infected plants (hereafter phyllosphere-resident isolates; Supplementary Table 9). These phyllosphere-resident isolates were obtained from Arabidopsis leaves simultaneously with the Hpa-associated isolates. We found that most of the HAM isolates reached significantly higher abundances when individually co-inoculated with gnoHpa than without it (Fig. 5a). In particular, the core HAM isolate represented by *Sphingobium* ASV

ed6be benefited greatly from gnoHpa presence as its abundance increased significantly to more than 1,000-fold in the presence of gnoHpa. The phyllosphere-resident isolates, however, were unaffected or even declined in abundance in the presence of gnoHpa. These results highlight that the HAM is specifically promoted in the phyllosphere by downy mildew infection.

In similar experiments, we quantified gnoHpa spore production and observed that HAM isolates *Aeromicrobium* d93fb and *Microbacterium* f0c76-2 significantly reduced gnoHpa spore production, whereas phyllosphere-resident isolates *Pseudomonas* fb830 and *Duganella* f90ae significantly promoted the production of gnoHpa spores (Fig. 5b). These results suggest that some HAM bacteria can aid the plant in reducing downy mildew disease. To further explore this, we quantified Hpa sporulation after inoculating *Arabidopsis* seedlings with Hpa or gnoHpa at multiple starting inoculum densities (Fig. 5c), with gnoHpa supplemented with either bacterial leaf wash-offs from Hpa-infected plants from which Hpa spores were removed through filtration (gnoHpa plus HAM; Fig. 5d) or with similarly treated leaf wash-offs from healthy plants (gnoHpa plus resident; Fig. 5e). Seven dpi, HAM-free gnoHpa produced more spores compared with regular HAM-containing Hpa (Fig. 5c,d). Interestingly, supplementation of gnoHpa with HAM wash-offs reduced spore production to the same level as regular HAM-containing Hpa (Fig. 5d). When we compared the effect of HAM with that of phyllosphere-resident microbiota from healthy plants on gnoHpa performance (Fig. 5e), we again observed a negative effect of HAM on gnoHpa spore production, while the phyllosphere-resident microbiota yielded even higher sporulation than HAM-free gnoHpa on its own (Fig. 5e).

Thus, HAM members reduce Hpa sporulation to promote host health. We propose that the HAM is a disease-suppressive, infection-associated microbiome.

Phyllosphere HAM is recruited from the rhizosphere

Previously, we showed that conditioning of soil (known as a soil-borne legacy¹⁸) by Hpa-infected *Arabidopsis* makes the next planting in that soil more resistant to Hpa¹³. This phenomenon is associated with a shift in the rhizosphere microbiome that mediates induced systemic resistance against Hpa in a next population of plants^{13,20}. Interestingly, a number of the ASVs that were enriched in the rhizosphere upon foliar Hpa infection¹³ were also found in the phyllosphere HAM in our study. We hypothesized that colonization of HAM bacteria occurs first in the rhizosphere upon foliar infection with Hpa, resulting in the creation of a soil-borne legacy. When a subsequent population of plants germinates in soil with a 'soil-borne legacy', their phyllospheres acquire the HAM bacteria, which upon foliar Hpa infection are further stimulated and become members of the HAM in the phyllosphere.

To test this hypothesis, we first set up a soil-borne-legacy experiment in which we conditioned soil with *Arabidopsis* Col-0 plants inoculated with mock, regular HAM-containing Hpa Noco2, or HAM-free gnoHpa Noco2, after which we quantified susceptibility of the successive (response) population of Col-0 plants on that soil to Noco2 (Extended data Fig. 5). Interestingly, Hpa sporulation was reduced on plants that were growing on soil conditioned by either Hpa-infected or gnoHpa-infected plants (Fig. 6a and Supplementary Fig. 15). This suggests that Hpa infection by itself, even without its associated HAM, is sufficient for the creation of a soil-borne legacy. To verify this further, we tested whether conditioning of the soil with Hpa-inoculated Col-0 *RPP5* plants, which are resistant to Hpa Noco2, would lead to the creation of a soil-borne legacy. This was not the case (Fig. 6b), confirming that Hpa infection is required for the establishment of a legacy and that introduction of HAM bacteria to the conditioning population of plants is not sufficient to create a soil-borne legacy.

Next, we tested whether the HAM bacteria that were promoted by Hpa-infected plants were subsequently picked up by a succeeding

population of plants growing in the conditioned soil. To this end, we monitored the build-up of HAM bacteria in the rhizospheres and the phyllospheres of conditioning-phase and response-phase Col-0 plants in the soil-borne legacy experimental set-up (Extended Data Fig. 5). As expected, 1 week after inoculation of the conditioning population of Col-0 plants with HAM-containing Hpa, we observed a significant shift in the phyllosphere bacterial community (Supplementary Fig. 16a; PERMANOVA: $R^2 = 0.58$, $P < 0.001$), while upon inoculation with HAM-free gnoHpa, we did not (Supplementary Fig. 16; PERMANOVA: $R^2 = 0.05$, $P = 0.45$). Using DESeq2 (ref. 26), we identified 52 ASVs that were uniquely enriched ($P < 0.05$; Supplementary Table 10) and together comprised 90% of the total bacterial community in the phyllosphere of Hpa-inoculated plants (Fig. 6c). The enriched ASVs were largely consistent with our earlier observations (Figs. 1, 2 and 4). In the remainder of this experiment, these 52 ASVs are collectively referred to as HAM ASVs. The HAM ASVs were present at low abundance or below the detection limit in the phyllosphere of mock- or gnoHpa-inoculated plants (Fig. 6c) and in the rhizospheres of all conditioning-phase plants (Fig. 6d), confirming that in the conditioning phase, they established in the phyllosphere as a result of co-inoculation with HAM-containing Hpa.

Subsequently, we monitored the build-up of the HAM bacterial phyllosphere and rhizosphere communities of soil-borne-legacy response-phase Col-0 plants, 1 week after inoculation of this second population of plants with HAM-free gnoHpa or a mock solution (Extended Data Fig. 5). Although no HAM bacteria were introduced during the inoculation of response-phase plants with gnoHpa, we found that the cumulative abundance of the HAM ASVs was substantially higher in the phyllospheres (Fig. 6e) and rhizospheres (Fig. 6f) of plants growing on Hpa-conditioned soils than on those growing on mock-conditioned soils. In the phyllosphere, *Xanthomonas* ASV a0e1a was among the most dominant HAM ASVs that were transferred by Hpa-conditioned soil to the response population of Col-0 plants (Fig. 6e), whereas in the rhizosphere, *Flavobacterium* ASV ef66d increased in abundance the most (Fig. 6f). Although we cannot be certain that these HAM ASVs represent bacteria isogenic to the isolates described above (Figs. 3 and 5), these results suggest that phyllosphere HAM bacteria are soil borne and that they can readily colonize the phyllosphere from Hpa-conditioned soil.

Remarkably, we observed that in the response population of gnoHpa-inoculated Col-0 plants growing on mock-conditioned soil, the cumulative relative abundance of HAM ASVs was significantly higher in both the rhizosphere and phyllosphere compared with that of mock-inoculated response-phase plants (Fig. 6e,f). Because in these gnoHpa treatments HAM bacteria were never introduced with the inoculum, we concluded that gnoHpa-inoculated plants specifically recruit HAM bacteria in both the rhizosphere and phyllosphere. Furthermore, the cumulative relative abundance of HAM ASVs was significantly higher in both the rhizospheres (Fig. 6g) and the phyllospheres (Fig. 6h) of response-phase plants that either grew on gnoHpa-conditioned soil or were inoculated with gnoHpa. These results further support the notion that HAM bacteria are selected for in the rhizosphere and phyllosphere of Hpa-infected plants.

Aeromicrobium and *Xanthomonas* are important HAMs

We then compared the abundance of ASVs between gnoHpa-inoculated plants on gnoHpa-conditioned soil and mock-inoculated plants on mock-conditioned soil. Ten HAM ASVs were among the top 30 most strongly enriched ASVs in the phyllosphere of gnoHpa-infected plants (Supplementary Fig. 17), underlining the selective recruitment of HAM ASVs by infected plants. The fourth most strongly responding ASV is *Xanthomonas* HAM ASV a0e1a, which increased 17-fold in phyllosphere abundance and 2.7-fold in the rhizosphere of gnoHpa-infected plants. Previously, we showed that *Xanthomonas* sp. WCS2014-13, representative of HAM ASV a0e1a, can contribute to suppression of Hpa¹³.

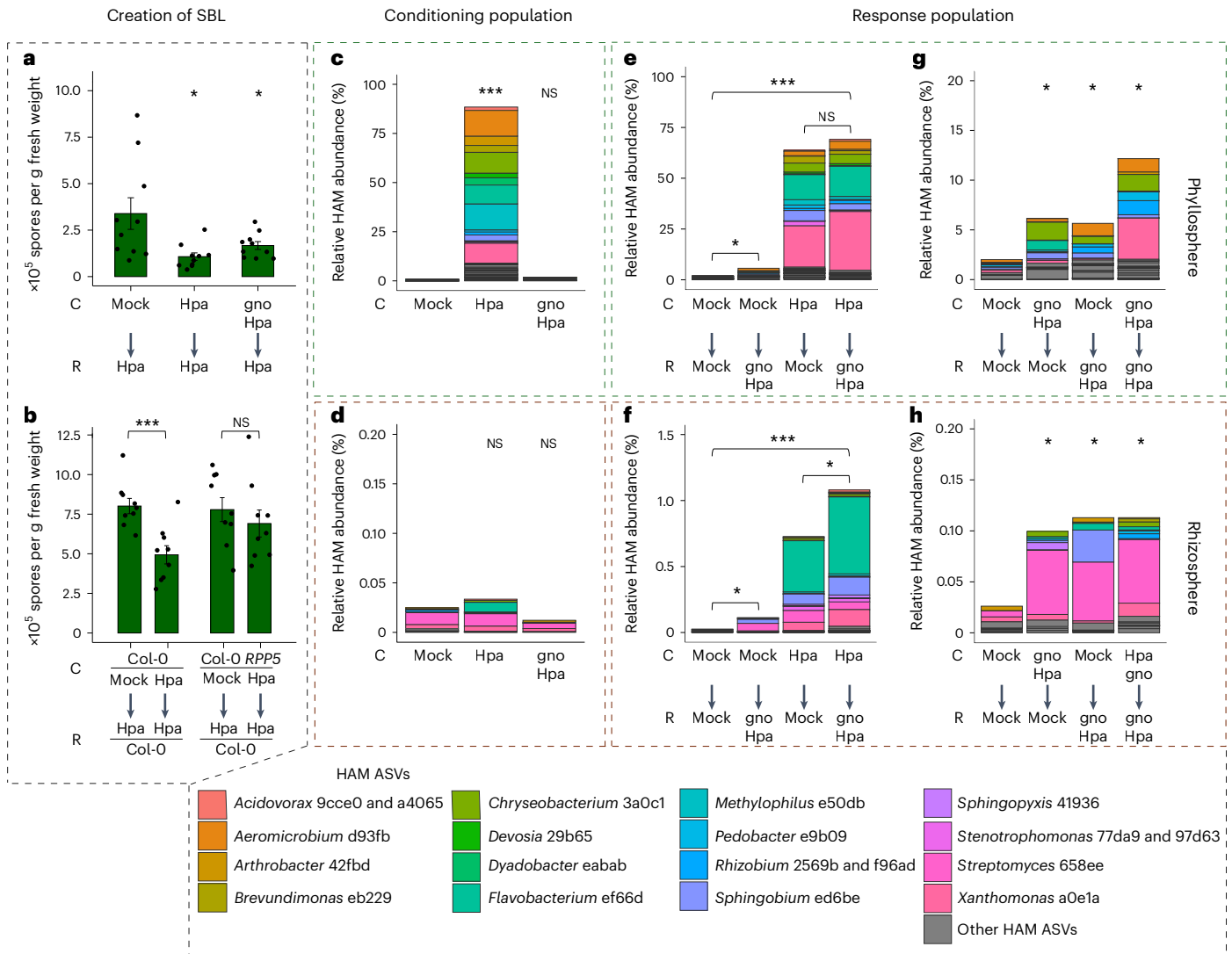


Fig. 6 | HAM ASVs are selectively promoted in response to Hpa infection and associated with soil-borne legacy. **a**, Hpa spore production in response (R) populations of Arabidopsis Col-0 plants growing on soil conditioned (C) by populations of Col-0 plants inoculated with either mock, Hpa or gnoHpa spore suspensions. Asterisks indicate significant differences between conditioned and mock-conditioned plants in FDR-corrected one-sided Student's *t*-test: (left to right) $*P = 0.016$; $*P = 0.033$. **b**, Hpa spore production of Arabidopsis Col-0 plants growing in soil conditioned by populations of Col-0 or transgenic Col-0 *RPP5* plants that had been mock inoculated or inoculated with an Hpa-spore suspension. Spore production was quantified 7 dpi and normalized to shoot fresh weight. Asterisks indicate significance level in one-sided Student's *t*-test comparing Hpa-conditioned with mock-conditioned plants per plant genotype: $***P = 4.2 \times 10^{-4}$; NS, not significant. **c–h**, Cumulative relative abundance of 52 HAM ASVs in the phyllosphere (**c, e, g**) or rhizosphere (**d, f, h**) of a conditioning (**c, d**) or response (**e, f, g, h**) population of Arabidopsis Col-0 plants. Colours indicate the taxonomy of 19 distinct HAM ASVs that together comprise the

top-15 most abundant HAM ASVs in the phyllosphere and rhizosphere. Colours correspond to single HAM ASVs, except for the genera *Acidovorax*, *Rhizobium* and *Stenotrophomonas* which are represented by two HAM ASVs. In **c**, asterisks indicate the significance level in FDR-corrected one-sided Student's *t*-test comparing treated with mock-treated plant populations: $***P = 3.9 \times 10^{-25}$. In **e** and **f**, asterisks indicate the significance level in one-sided Student's *t*-test comparing Hpa-conditioned with mock-conditioned soils and gnoHpa-inoculated with mock-treated plant populations: $***P = 4.6 \times 10^{-21}$; $*P = 0.041$ (**e**), and (left to right) $*P = 0.010$; $***P = 9.8 \times 10^{-12}$; $*P = 0.019$ (**f**). In **g** and **h**, asterisks indicate the significance level in FDR-corrected one-sided Student's *t*-test comparing treated with mock-treated, and conditioned with mock-conditioned, plant populations: (left to right) $*P = 0.035$; $*P = 0.041$; $*P = 0.035$ (**g**); $*P = 0.015$ (for all three asterisks) (**h**). All bars and error bars indicate the average and standard error, respectively, of ten biological replicates, except for **b** (nine replicates) and **d** gnoHpa (eight replicates).

Although the enrichment of the predefined HAM ASVs was evident, the increase of most HAM ASVs was not statistically significant as a result of their irregular occurrence and consequential low statistical power. To deal with the sparsity of 16S rDNA amplicon data, we used Analysis of Compositions of Microbiomes with Bias Correction (ANCOM-BC)³⁴ for differential abundance testing. Nonetheless, in the rhizosphere, ANCOM-BC identified only a single non-HAM ASV that was significantly enriched (FDR-adjusted $P < 0.05$). Also, in the phyllosphere, the enrichment of only 1 of 452 phyllosphere ASVs was found statistically significant by ANCOM-BC following infection. However,

this single significantly responding ASV was *Aeromicrobium* HAM ASV d93fb (Supplementary Fig. 18). Extraordinarily, the isolate representing specifically this HAM ASV consistently reduced spore production when co-inoculated with gnoHpa on axenic Arabidopsis plants (Fig. 5b). The observed phyllosphere enrichment of *Aeromicrobium* ASV d93fb and *Xanthomonas* ASV a0e1a resulting from gnoHpa infection could thus be sufficient to explain the increased resistance associated with soil-borne legacy. Together, these results again highlight that HAM ASVs are specifically promoted as a result of gnoHpa infection and suggest that the increased resistance conferred by soil-borne legacy results

from the increased abundance of HAM bacteria and their combined actions in the phyllosphere.

Discussion

Here, we investigated whether infection by a foliar pathogen leads to changes in the phyllosphere microbial community. We found that cultures of distinct isolates of the obligate downy mildew pathogen Hpa strictly separately maintained in research institutes in Germany, the Netherlands and the United Kingdom are associated with a set of isogenic Hpa-associated bacteria. Most prevalent among these phyllosphere HAM bacteria is a *Xanthomonas* sp. that was found in 7 out of 11 Hpa cultures, but isogenic representatives of at least 6 out of 9 HAM isolates were frequently represented in the Hpa cultures that we investigated. Our results show that a HAM community is selectively promoted in the phyllosphere of Hpa-infected plants and that this can be reconstructed on axenic Arabidopsis plants on which HAM-free gnoHpa and individual HAM isolates are co-inoculated. Interestingly, inoculation of Arabidopsis plants growing on natural soil with HAM-free gnoHpa resulted in increased relative abundances of HAM ASVs in both the rhizosphere and phyllosphere of infected plants. We provide evidence that HAM bacteria are recruited from the soil surrounding downy-mildew-infected plants to the phyllosphere of a next population of plants growing in the conditioned soil, where they are subsequently further promoted by Hpa infection. The fact that isogenic bacteria are members of HAM communities in physically and geographically separated Hpa cultures suggests that these specific HAM members are independently selected from different soils by Arabidopsis in response to Hpa infection. In an analogy to the Baas Becking hypothesis “Everything is everywhere, but the environment selects”³⁵, it seems that HAM bacteria are everywhere, but the infected plant selects.

In recent years, evidence has mounted that upon perceiving environmental stress, plants recruit a specific microbiome to help alleviate effects of stressors such as nutrient deficiency^{36,37}, drought^{38–40} or salinity⁴¹ and also microbial pathogens^{8,13,14,21,42}. The disease-induced recruitment of beneficial microorganisms has also been hypothesized to result in the creation of disease-suppressive soils^{18,19,21,22,43–45}.

While HAM growth is promoted on Hpa-infected leaves, Hpa spore production is reduced by the HAM. Therefore, the HAM is an infection-associated microbiome that protects the host. Moreover, foliar Hpa infection can stimulate a soil-borne legacy that results in increased resistance to Hpa of a subsequent population of plants growing on the same soil. This increased resistance also coincides with an increased cumulative abundance of HAM ASVs in the rhizosphere and phyllosphere of these plants. As the application of HAM isolates to leaves (this study) or to roots¹³ is sufficient to reduce Hpa spore production, it is likely the HAM is responsible for the increased protection that results from soil-borne legacy. The mechanism by which HAM either directly or indirectly protects against Hpa requires further investigation. However, we previously found that mutant plants impaired in defence signalling, which involves the plant hormone salicylic acid, are not protected by an Hpa-induced soil-borne legacy, suggesting that soil-borne legacy and HAMs work at least partly through activation of salicylic-acid-dependent immunity²⁰.

We report here that Arabidopsis plants that are infected by the downy mildew pathogen develop infection-associated microbiomes in the phyllosphere and in the rhizosphere. This infection-associated microbiome hinders pathogen development and is therefore the opposite of a pathobiome^{46,47}, which promotes pathogen infection. Whereas the microbiome directly associated with propagules of fungal pathogens can also limit pathogen proliferation⁴⁸, our results suggest that it is not Hpa itself that promotes Hpa-infection-associated microbiome assembly. Hpa spores do not carry HAM bacteria. Moreover, the creation of a soil-borne legacy requires infection by the pathogen, as resistant plants that Hpa cannot infect did not result in a soil-borne legacy. Previously, we reported that foliar Hpa infection changes the

root exudation profile and that mutant plants impaired in the biosynthesis of root-secreted coumarins are not able to create a soil-borne legacy even though they are just as susceptible as the wild type²⁰. This indicates that it is likely that the plant actively assembles this infection-associated microbiome in response to pathogen attack.

Future research is needed to elucidate the plant genetic mechanisms underlying microbiome recruitment. A fundamental understanding of these mechanisms might enable breeding of crop varieties that actively assemble protective microbiomes.

Methods

Plant materials and growth conditions

In this study, we used the Arabidopsis accessions Col-0, Ler, C24²⁷ and Pro-0²⁸; transgenic Col-0 *RPP5* plants²⁵; and the mutants Ler *rpp5*³³ and *edsI*^{4,49}. For the experiments performed at Utrecht University that correspond to results shown in Figs. 1, 2 and 4, 60 ml pots were filled with approximately 90 g of a mix of river sand and potting soil (5:12) supplemented with 10 ml half-strength Hoagland solution⁵⁰ and further saturated with water. Twenty-one seeds were sown on top of the soil using toothpicks (Figs. 1–3) or denser fields of seedlings were sown through gentle dispersion from seed bags (nine-passage experiment; Fig. 4). Pots with seeds were subsequently submitted to stratification for 3 days in the dark at 4 °C. Seeds were then allowed to germinate and develop in a climate-controlled chamber (21 °C, 70% relative humidity, 12 h light and 12 h dark, light intensity 100 $\mu\text{mol m}^{-2} \text{s}^{-1}$). For the experiments at the Max Planck Institute for Plant Breeding Research, Cologne, seeds were stratified for 3 days in the dark at 4 °C, sown on water-saturated Jiffy pellets (J-7) and allowed to develop at slightly shorter day cycles (10 h light and 14 h dark). For experiments in which multiple genotypes of Arabidopsis were used simultaneously, seeds were surface sterilized before sowing by vapour-phase sterilization as described previously⁵¹.

For bioassays with both Hpa and gnoHpa and for soil-borne-legacy experiments (Figs. 5 and 6), natural soil from the Reijerscamp nature reserve (52.0107° N, 5.7825° E) in the Netherlands¹³ was used. The soil was air-dried and sieved twice (1 × 1 cm²) to remove rocks and plant debris. One day before sowing, the soil was watered in a 1:10 v/w ratio. Pots with a volume of 60 ml were filled with 120 g of soil (± 2.5 g), placed in 60 mm Petri dishes, and the soil surface was covered with a circular cutout of plastic micropipette-tip holders (Greiner Bio-One, 0.5–10 μl , item number 771280) to prevent growth of algae and to ensure that seeds are equally distributed during sowing⁵². Pots were stored at 4 °C overnight before sowing. Arabidopsis accession Col-0 seeds were suspended in 0.2% (w/v) agar solution and stratified in dark conditions at 4 °C for 48–72 h. Seeds were sown by pipetting two or three seeds per hole of the plastic cover, resulting in approximately 30 seeds per pot. After sowing, pots were stored in trays with transparent lids and put in a growth chamber (21 °C, 70% relative humidity, 10 h light and 14 h dark, light intensity 100 $\mu\text{mol m}^{-2} \text{s}^{-1}$). Pots were watered two times a week with 3 ml water. After 1 week, closed lids were replaced with meshed lids to reduce humidity and plants were watered once with 5 ml of half-strength Hoagland nutrient solution.

Preparation of Hpa spore suspensions and inoculation of plants

Hpa spore suspensions were prepared by collecting shoot material 7–14 days after inoculation with spore suspensions of Hpa isolate Noco2 (ref. 25) or Cala2 (ref. 24) and by vigorously shaking the material in 20 ml of autoclaved tap-water. Spores were counted in three separate 1 μl droplets using a transmitted-light microscope (Carl Zeiss Microscopy, Standard 25 International Classification for Standards, item number 450815.9902), and subsequently, the spore suspensions were diluted to obtain appropriate spore densities as specified below.

For the experiment performed in Utrecht that corresponds to data shown in Figs. 1 and 2, and Supplementary Fig. 1, 10-day-old Arabidopsis seedlings were spray inoculated with spore suspensions in

autoclaved tap-water containing Hpa isolate Noco2 or Cala2 (50 spores per μl) or a mix of both spore suspensions (50 spores per μl of each isolate), or mock-treated with autoclaved tap-water. Wind inoculations of Noco2 were performed by placing a pot with healthy 10-day-old Col-0 plants below a pot of Hpa-inoculated and heavily sporulating plants that was held at a 90° angle, and spores were dispersed from the sporulating plants by a brief pulse of compressed air from above. In Cologne (experiment corresponding to Fig. 2), 16-day-old Arabidopsis seedlings were spray inoculated with Noco2 or Cala2 spores in Milli-Q water or mock inoculated with Milli-Q. In bioassays and soil-borne legacy (SBL) experiments (Figs. 5 and 6), 14-day-old seedlings were spray inoculated with Hpa or gnoHpa spore suspensions in tap-water (Fig. 5c, 10, 25, 50 and 100 spores per μl ; Fig. 5d,e, 25 spores per μl ; Fig. 6a, 50 spores per μl ; Fig. 6b, 85 spores per μl). Pots with inoculated plants were air-dried and randomly placed in trays in a climate chamber (16 °C, Figs. 1–4; 21 °C, Figs. 5 and 6; 10 h light and 14 h dark, light intensity 100 $\mu\text{mol m}^{-2} \text{s}^{-1}$) and were covered with moisturized transparent lids to increase humidity.

Arabidopsis sample collection and disease quantification

Seven days after inoculation with Hpa spore suspensions, infected Arabidopsis shoot material was collected in 2 ml Eppendorf tubes (Utrecht; Figs. 1, 2, 4 and 6) or 15 ml conical tubes (Cologne; Fig. 2) containing three glass beads, carefully avoiding the sampling of roots or soil.

For DNA isolation, the material was immediately snap-frozen in liquid nitrogen and stored at –80 °C until further processing. Rhizosphere samples were taken by gently sieving the pots under running tap-water until the loosely adhering soil was washed away and only roots with attached soil were left. For bulk soil samples, the upper soil layer (± 2 cm) was removed and the exposed soil was sampled. All sample types were collected in 2 ml Eppendorf tubes, snap-frozen in liquid nitrogen and stored at –80 °C until further processing. DNA from the Cologne samples was isolated in Cologne.

For disease quantification, the weighted shoot material was suspended in 3–6 ml of water depending on fresh weight and level of observed sporulation. Greiner tubes were vortexed for 15 s, and spores were counted in three separate 1 μl droplets using a transmitted-light microscope (Carl Zeiss Microscopy, Standard 25 International Classification for Standards, item number 450815.9902); the average spore count was normalized by shoot fresh weight.

Genomic DNA extractions

Total genomic DNA (gDNA) was extracted from Arabidopsis leaves and resident microbiomes using the PowerLyzer PowerSoil DNA isolation kit (Qiagen) modified for leaf material. In brief, frozen leaf samples were mechanically lysed twice for 60 s at 30 Hz using the TissueLyser II (Qiagen). Per sample, 750 μl of Powerbead solution and 60 μl of C1 solution were added; samples were mixed by inverting tubes and subsequently incubated for 10 min at 65 °C. Total solutions were then transferred to Powerbead tubes and submitted to bead beating, twice, for 10 min at 30 Hz. Samples were then centrifuged for 4 min at 10,000 $\times g$, and the supernatant was transferred to new 2 ml collection tubes. The protocol was subsequently completed without further modifications according to the manufacturer's instructions. DNA extractions for phyllosphere samples from the SBL experiment were performed using the Qiagen MagAttract PowerSoil DNA KF Kit and a Thermo Fisher KingFisher with the same modifications for leaf material as described above. Rhizosphere and bulk soil DNA was extracted according to the protocol provided by the Qiagen MagAttract PowerSoil DNA KF Kit. All DNA concentrations were quantified using a NanoDrop 2000.

Hpa quantification by quantitative real-time PCR

Hpa was quantified from gDNA obtained from Hpa-infected and uninfected Arabidopsis shoot material according to a previous study⁵³. Two-step quantitative real-time PCRs were performed in optical 96-well

plates with a ViiA 7 real-time PCR system (Applied Biosystems), using Power SYBR Green PCR Master Mix (Applied Biosystems) with 0.8 μM primers (Supplementary Table 11). A standard thermal profile was used: 50 °C for 2 min, 95 °C for 10 min, 40 cycles of 95 °C for 15 s and 60 °C for 1 min. Amplicon dissociation curves were recorded after cycle 40 by heating from 60 °C to 95 °C with a ramp speed of 1.0 °C⁻¹. Hpa abundance was calculated by $2^{-(\text{CtHpaACTIN} - \text{CtArabidopsisACTIN})}$, in which CtHpaACTIN and CtArabidopsisACTIN are the cycle threshold (Ct-) values obtained within samples for the ACTIN PCR products for Hpa and Arabidopsis, respectively.

16S rDNA amplicon library preparation for microbiome analysis

For the amplicon sequencing of the experiment in Fig. 1 and Supplementary Fig. 1, library preparations for Illumina 16S rDNA and ITS2 amplicon sequencing were performed on gDNA samples using standard materials and methods as described in the Illumina protocol. For amplicon sequencing of experiments corresponding to results shown in Figs. 2 and 4, we used primers with heterogeneity spacers for the 16S amplicon PCR⁵⁴. This change was implemented to increase nucleotide diversity in the first 25 bases as analysed by MiSeq and lower the required amount of PhiX⁵⁴ spike-in, thereby increasing read depth per sample (Supplementary Table 11). All 16S rDNA library preparations were performed with the addition of peptide nucleic acid PCR clamps to the PCR1 reaction mixtures, at 0.25 μM per reaction, to prevent the amplification of plant-derived sequences⁵⁵. ITS2 amplicon libraries were prepared in similar fashion, using primers⁵⁶ and blocking oligonucleotides as specified in Supplementary Table 11, with altered numbers of PCR cycles (PCR1, 10 cycles; PCR2, 25 cycles), to accommodate the use of the ITS2 blocking oligonucleotides for the prevention of plant-derived reads⁵⁷. Sequencing was performed with MiSeq V3 chemistry (2 \times 300 base pairs paired-end sequencing) at the Utrecht Sequencing Facility (USEQ, Utrecht, the Netherlands; Figs. 1, 2 and 4).

For amplicon sequencing of the SBL experiment (Fig. 6), library preparation and sequencing with NovaSeq chemistry (2 \times 250 base pairs paired-end sequencing) was performed using Genome Quebec (Quebec, Montreal, Canada). The primers used were 16S-B341F (5'-CCTACGGGNGGCWGCAG) and 16S-B806 (5'-GACTACHVGGGTATCTAATCC) according to Genome Quebec's standard operating protocols. Plastid- and mitochondrial-blocking peptide nucleic acids (pPNA, 5'-GGCTCAACCTGGACAG, and mPNA, 5'-GGCAAGTGTCTTCGGA, respectively) were used in the PCRs to prevent amplification of plant-derived sequences.

16S rDNA and ITS2 amplicon sequencing analyses

Preprocessing of sequencing data was performed in the Qiime2 environment (version 2019.7)⁵⁸, using Cutadapt⁵⁹ to remove primer sequences from reads and DADA2 (ref. 60) for quality filtering, error correction, chimera removal and dereplication to ASVs. Samples from the SBL experiment (Fig. 6) were sequenced twice, and the resulting two datasets were merged after Cutadapt and DADA2 processing. ASV identifiers were assigned based on the sequence-specific MD5-sums using the `-p-hashed-feature-ids` parameter, of which we used the first five characters in the text above to designate the individual ASVs. For 16S rDNA datasets, taxonomic assignment was performed using the VSEARCH plugin and the SILVA database (QIIME-compatible 138-release, 99% clustering identity, seven-level Ribosomal Database Project-compatible consensus taxonomies) from which the 16S variable regions 3 and 4 were extracted based on the 16S rDNA specific primer sequences used in library preparation. Plant-derived sequences were identified and removed based on the annotation of 'D_4_Mitochondria' at the family level or 'D_2_Chloroplast' at the class level. Additionally, ASVs with unassigned taxonomies were removed.

In the experiments sequenced with the MiSeq platform, ASVs in the lowest 1% (Figs. 1, 2 and 4) or the lowest 3% (Supplementary Fig. 1b)

of total cumulative abundances were removed. For the sequencing data generated with the NovaSeq platform, ASVs that contribute to the lowest 3% of total cumulative abundance or that were detected in fewer than five samples were removed from the data (Fig. 6). This resulted in a dataset comprising 651,957 reads and 391 ASVs in 20 samples (Supplementary Fig. 1b), a dataset comprising 3,202,185 reads and 454 ASVs in 61 samples (Utrecht experiment; Fig. 1), a dataset comprising 4,384,956 reads and 458 ASVs in 47 samples (Cologne experiment; this ASV table was merged with the Utrecht experiment resulting in an ASV table with a total of 841 ASVs and 7,587,141 reads used in Fig. 2), a dataset comprising 13,310,029 reads and 1,151 ASVs in 93 samples (Fig. 4) and, finally, 31,340,888 reads and 4,241 ASVs in 240 samples (Fig. 6). Fungal ITS amplicons were taxonomically classified using a fitted classifier trained on the UNITE fungal database (QIIME release, version 7.2, 99% similarity clustering, seven-level taxonomies). ITS2 sequences (ASVs) with a total cumulative abundance of fewer than 63 reads were filtered out, and samples with fewer than 1,000 reads were removed from the dataset, resulting in 264,468 reads comprising 130 ASVs in 19 samples (Supplementary Fig. 1c).

All beta-diversity-related calculations, graphs and differential abundance tests were performed in R (version 4.0.3). All PCoA ordinations and PERMANOVA tests were performed on Bray–Curtis dissimilarity matrices calculated for relative abundance data, using either *vegan* (version 2.5.7) or *vegan* functionalities within the *phyloseq* package (version 1.34.0). The *pairwiseAdonis* package (version 0.0.1) was employed for PERMANOVA tests involving multiple comparisons. For the SBL experiment (Fig. 6), rhizosphere samples R-G-G1-4 and R-G-G1-8 clustered away from the other rhizosphere samples towards bulk soil samples. Hence, these samples were considered not representative of the rhizosphere and removed for downstream analysis. Differential abundance testing was performed with either ANCOM-BC³⁴ or DESeq2 (ref. 26; version 1.30.1), employing a separate function to calculate the geometric mean used for the *estimateSizeFactor* step, namely, $\text{function}(x, \text{na.rm}=\text{TRUE}) \exp(\text{sum}(\log(x[x > 0])), \text{na.rm}=\text{na.rm}) / \text{length}(x))$ (described in <https://bioconductor.org/packages/devel/bioc/vignettes/phyloseq/inst/doc/phyloseq-mixture-models.html>). This circumvents errors related to the sparsity in 16S rDNA amplicon data. Dendrogram visualization for Fig. 3b was achieved using the interactive tree of life (ITOL) webtool (<https://itol.embl.de/>). All other graphs were made using *ggplot2* (version 3.3.3) or *ggpubr* (version 0.4.0). Data wrangling was done with packages from the Tidyverse suite.

Bacterial isolate collection

Infected shoot material was collected from Noco2- and Cala2-infected plants in Utrecht in 2018 and in Cologne in 2017 and 2019. Shoot material of Hpa-infected plants was stored in 1 ml of 10 mM MgSO₄ with 25% glycerol (v/v) at –80 °C. For isolation, shoots were defrosted in Utrecht at room temperature and plants were crushed using sterile pestles. To maximize the isolation of culturable bacterial species, a dilution series of the Utrecht samples was plated on agar-solidified medium containing either one-tenth-strength tryptic soy broth (TSB; Difco), King's medium B⁶¹ amended with 13 mg l⁻¹ chloramphenicol and 40 mg l⁻¹ ampicillin (KB +), Luria–Bertani (Difco), R2A (Difco), yeast extract mannitol (per litre: 0.5 g yeast extract (Difco), 5 g mannitol, 0.5 g K₂HPO₄, 0.2 g MgSO₄·7H₂O, 0.1 g NaCl (Difco), pH 7.0), nutrient agar (per litre: 5 g peptone (Difco), 3 g beef extract (Difco), pH 6.8) and glucose nutrient agar (per litre: 5 g peptone, 3 g beef extract (Difco), 10 g glucose (Difco)). All media were amended with 200 µg ml⁻¹ Delvocid (DSM; active compound, natamycin) to prevent fungal growth. Plates were incubated at 21 °C for 2–11 days. A total of 654 bacterial colonies, selected on morphology and/or time of emergence, were streaked on the same type of agar medium from which they were selected. Single colonies from pure cultures were inoculated in one-tenth-strength TSB (Difco), incubated overnight at 20 °C and 180 rpm, and stored

at –80 °C in 25% (v/v) glycerol. Pure cultures were labelled based on the sample they originated from and the type of medium they were isolated from, and numbered according to the order of selection on that medium. Similar methods were applied to isolate xanthomonads from the Cologne samples, but only one-tenth-strength tryptic soy agar (TSA) was used and 48 colonies were selected for yellow colour of colonies.

Initial characterization of bacterial isolates

All isolates were processed for simultaneous 16S rDNA sequencing using Illumina MiSeq V3 chemistry, using the multiplexing strategy described in a previous study⁵⁴. All isolates were grown for 2 days in one-tenth-strength TSB, and 1 µl of each culture was added directly to a PCR in 96-well plates, containing 0.2 µM of column-specific forward primers and row-specific reverse primers (Supplementary Table 11), and 2× KAPA HiFi Hotstart Ready Mix (Roche) to a total volume of 15 µl. PCR was performed by 10 min incubation at 95 °C followed by 30 cycles of 30 s at 95 °C, 30 s at 55 °C and 30 s at 72 °C, followed by a final elongation step of 5 min at 72 °C. PCR products were purified using AMPure XP beads with 9 µl of bead solution per 15 µl PCR mixture and washing with 80% ethanol. PCR products were quantified using a Nanodrop 2000 spectrophotometer (Thermo Fisher Scientific), concentrations were normalized to 1 ng µl⁻¹ and each 96-well plate of samples was combined into a pooled sample. Per pooled sample, 1 µl was then submitted to a second PCR, wherein each pooled sample was assigned its unique pair of Nextera indexing primers (Supplementary Table 11). These PCRs were performed with 2× KAPA HiFi Hotstart Ready Mix and 0.4 µM forward and reverse primers, in total volumes of 25 µl. The PCR products were purified as described above, quantified using the Qubit dsDNA BR Assay kit according to the manufacturer's instructions, normalized to 1 ng µl⁻¹ and again pooled together into a single 16S library. The 16S library was submitted to sequencing at USEQ. Between-plate demultiplexing was performed by USEQ, whereas within-plate demultiplexing and removal of adapters were achieved using *Cutadapt*⁵⁹. Sequence data per bacterial isolate were then processed in the *Qiime2* (ref. 58) environment using *DADA2* (ref. 60) as described above. The resulting ASVs were matched to ASVs from the 16S rDNA analyses of bacterial communities based on their sequence-specific MD5-sum identifiers.

Whole-genome sequencing of bacterial isolates

Whole-genome sequencing (WGS) of bacterial isolates was performed on gDNA that was extracted using the GenElute Bacterial Genomic DNA Kit according to the manufacturer's instructions. gDNA samples were processed for WGS at the Microbial Genome Sequencing Center (Pittsburgh, USA) and sequenced to an estimated coverage of 60× using 2 × 150 paired-end sequencing. Sequences from paired FASTQ files were quality filtered using *Trimmomatic*⁶² (version 0.39) with *SLIDINGWINDOW:4:20* as the only set parameter. Genomes were then assembled using *Spades*⁶³ (version 3.11.1) with ‘-careful’ as the only set parameter. Assemblies were checked using *Quast*⁶⁴. Contigs shorter than 1,000 bp were then removed using the Galaxy webserver (<https://usegalaxy.eu>) using the ‘filter fasta’ function. If genomes for multiple isolates per ASV were obtained, their ANIs were calculated using the *python3* module *pyani*. Dendrograms based on whole genomes were calculated using *mashtree* and visualized using the ITOL webserver (<https://itol.embl.de/>).

Analysis of publicly available Hpa metagenomes

Sequence data described in a previous study³⁰, which were obtained from Emoy2 spores collected in water (similar to the Hpa inocula used in our study), were obtained in fasta format from the NCBI TRACE archive using query ‘species_code = ‘HYALOPERONOSPORA PARASITICA’. The first and the last 100 base pairs of all reads were removed using *Trimmomatic*, resulting in reads with an average length of approximately 600 bp.

Sequence data described in a previous study³¹ were obtained from the European Nucleotide Archive under project number PRJEB22892. These reads were filtered based on quality using Trimmomatic, using SLIDINGWINDOW:4:20 and MINLEN:45 for fastq files with 2×60 bp and 2×75 bp reads, and SLIDINGWINDOW:4:20 MINLEN:30 for fastq files with 2×35 bp reads.

To quantify specific genomes of interest within their respective genera, first, we obtained non-redundant genomes of genera of interest, using bacsort (<https://github.com/rwick/Bacsort>), which picks the best genome assembly from clusters of genomes that are within 98% ANI (with parameter $-\text{threshold } 0.02$) of each other. Kallisto indices^{32,65} were then built using all these non-redundant genomes, the genomes of the bacteria identified and sequenced in the study, the Hpa Emoy2 genome and the Arabidopsis genome. All reads per Hpa metagenome were then pseudo-aligned³² against these indices, and the proportion of reads that pseudo-aligned to the genome of interest among all reads mapped to genomes within that genus was calculated (Supplementary Figs. 4–11). Signal-to-noise ratios were calculated (Fig. 3a), in which signal represents the number of reads that were assigned to a specific genome, and noise was calculated as the total number of reads that were assigned to all genomes within a specific genus, divided by the number of genomes within that genus (as included in the genome index).

Nine-passage experiments

Ten pots with 10-day-old seedlings of Arabidopsis accessions Col-0 and Ler, and transgenic Col-0 *RPP5*²⁵, provided by J. Parker (Max Planck Institute for Plant Breeding Research, Cologne, Germany) were inoculated with a mix of Noco2 and Cala2 spore suspensions, prepared as described above. These pots were placed in a tray covered with a transparent plastic lid, which was sprayed with water on the inside to raise humidity inside the tray, and the tray was placed in a climate chamber (16°C , 10 h light and 14 h dark, light intensity $100 \mu\text{mol m}^{-2} \text{s}^{-1}$). Hpa started to sporulate on Col-0 and Ler plants approximately 5 days after inoculation.

After 7 days, leaf wash-offs were obtained from each pot (30 pots in total) and used to spray-inoculate a population of 10-day-old Ler *rpp5*³³ (also provided by J. Parker, Cologne) plants growing on 60 ml pots, each of which was placed in an individual Eco2box. After 7 days, and visual and microscopic confirmation that sporulation occurred only in plants inoculated with Noco2 or Cala2, half of the seedlings per pot were collected, snap-frozen in liquid nitrogen and stored for further processing. The remaining plants from each pot were used to generate leaf wash-offs in 5 ml of autoclaved water, of which approximately 600 μl was spray inoculated onto a new population of 10-day-old Ler *rpp5* seedlings using 2 ml spray units, such that the leaf wash-off from one pot was used to inoculate the plants on one new pot only. These pots were again placed in new individual Eco2boxes to prevent cross-contamination and ensure the propagation of separated phyllosphere cultures. In total, this process was repeated eight times, thus passaging the Hpa-associated microbiome over nine consecutive Ler *rpp5* plant populations in the presence of either Noco2 (lineage 1) or Cala2 (lineage 2), or neither of the Hpa isolates (lineage 3). For each plant population in the nine-passage experiment, eight additional replicate pots with Ler *rpp5* plants were left untreated and collected as untreated controls. A schematic overview of this experiment is presented in Extended Data Fig. 3.

Creation of a gnotobiotic Hpa culture

Microbial contaminant-free Hpa (gnoHpa) was generated by successive passaging of Hpa isolate Noco2 to susceptible Arabidopsis Col-0 seedlings grown on Murashige and Skoog (MS; Duchefa Biochemie)⁶⁶ agar-solidified medium without sucrose. Vapour-phase sterilized⁵¹ Col-0 seeds were sown on MS agar medium. After 2 days of stratification at 4°C , Petri dishes were placed vertically in a growth chamber (21°C , 70% relative humidity, 12 h light and 12 h dark, light intensity

$100 \mu\text{mol m}^{-2} \text{s}^{-1}$). Ten-day-old axenically grown seedlings were then inoculated with Hpa (Noco2) by gently touching their leaves with sporangiophores extending from an Hpa-infected leaf in a sterile laminar-flow cabinet. This initial infection of axenically grown Col-0 seedlings was performed using Hpa-infected leaves from the standard (microorganism-rich) Utrecht laboratory culture of Noco2. Petri dishes with infected seedlings were then placed in a growth chamber with optimal conditions for Hpa infection (16°C , 10 h light and 14 h dark, light intensity $100 \mu\text{mol m}^{-2} \text{s}^{-1}$). Using the same gentle-touch-inoculation method, this Hpa culture was then passaged weekly to new axenically grown Col-0 seedlings on MS agar-solidified medium (stratified, germinated and grown as described above). After Hpa touch inoculations, newly infected axenically grown plants were placed in a growth chamber (16°C , 10 h light and 14 h dark, light intensity $100 \mu\text{mol m}^{-2} \text{s}^{-1}$). After each disease cycle, the absence of microbial contaminants was tested by serial dilution plating on one-tenth TSA. Following the observation that there were no culturable microorganisms present in the gnotobiotic culture, which required three passages, we double checked the gnotobiotic nature of these cultures using amplicon sequencing of the 16S rRNA gene as described above (data not shown). Upon verification of the absence of microbial contaminants, weekly passaging was performed on axenically grown hypersusceptible *eds1* (enhanced disease susceptibility 1) mutant seedlings^{4,49}, germinated and grown on MS agar medium as described above for Col-0, to increase spore inoculum densities.

Co-inoculation of gnoHpa and individual bacterial isolates on axenic plants

For gnotobiotic bioassays, vapour-phase-sterilized⁵¹ Col-0 seeds were sown on agar-solidified Hoagland medium⁵⁰ ($\text{pH} = 5.5$, 0.6% agarose w/v) in 24-well microtitre plates (one seedling per well), stratified at 4°C for 2 days and subsequently cultivated at 21°C , 70% relative humidity, 12 h light and 12 h dark, and light intensity $100 \mu\text{mol m}^{-2} \text{s}^{-1}$.

Bacterial isolates were grown on one-tenth-strength TSA plates for 2–3 days, depending on growth speed, at 28°C . Bacterial suspensions were then prepared by scraping colonies from the TSA agar medium into sterile MgSO_4 (10 mM), optical density was measured at 600 nm and the suspension was diluted to $\text{OD}_{600} = 0.2$ in MgSO_4 . GnoHpa suspensions were prepared by shaking 10–20 sporulating *eds1* mutant plants in 2 ml MgSO_4 and then transferring the suspension to a new 2 ml tube. Mixtures of gnoHpa and MgSO_4 , gnoHpa and bacteria, and MgSO_4 and bacteria were prepared at 9:1 ratio so that gnoHpa spore densities were ~ 150 spores per μl and bacterial densities were $\text{OD}_{600} = 0.02$. Leaves of 10-day-old Col-0 seedlings were then inoculated with these mixtures. For each seedling, both cotyledons and the first two true leaves were inoculated with a 0.3 μl droplet of suspension. Bacterial densities were quantified 7 dpi by tenfold serial dilution plating on one-tenth-strength TSA plates and counting colony-forming units. GnoHpa spore production was quantified 7 dpi as described above. Although all nine representative HAM bacterial isolates (Supplementary Table 9) were tested, no useful data on bacterial densities were obtained for *Rhizobium* (ASV 2569b) isolate WCS2018Hpa-8 owing to contamination of the assay.

Complementation of gnoHpa spores with the Hpa-associated microbiome

Hpa spore suspensions were prepared from Hpa and gnoHpa of isolate Noco2 as describe above. Half of the Hpa suspension was filtered using a sterile 10 μm filter, moistened in advance with autoclaved demineralized water, to remove Hpa spores and allow the passage of HAM bacteria. The absence of spores in the HAM filtrate was confirmed by microscopy and by spraying the filtrate directly onto susceptible plants, following which no sporulation was observed. Using an equal amount of leaf material from healthy Arabidopsis plants, we also obtained a suspension of phyllosphere-resident bacteria. The

bacterial HAM and phyllosphere-resident filtrates were subsequently supplemented with equal densities of gnoHpa spores.

We then spray inoculated ten replicate 60 ml pots with 14-day-old *Arabidopsis* Col-0 plants with 12.5 ml spore suspensions of Hpa or of gnoHpa mixed with water, HAM filtrate or resident filtrate. Plants were air-dried for 2 h, covered with transparent lids to ensure high humidity and incubated (21 °C, 10 h light and 14 h dark, light intensity 100 $\mu\text{mol m}^{-2} \text{s}^{-1}$). Seven dpi, Hpa and gnoHpa sporulation was quantified as described above.

Soil-borne-legacy experiment

Fourteen-day-old Col-0 or transgenic Col-0 *RPP5* plants growing on Reijerscamp soil were inoculated with spores of regular Hpa cultures or gnoHpa cultures of isolate Noco2 or mock inoculated as described above. Plants were air-dried for 2 h, covered with transparent lids to ensure high humidity and incubated (21 °C, 10 h light and 14 h dark, light intensity 100 $\mu\text{mol m}^{-2} \text{s}^{-1}$). Seven dpi of this conditioning population of plants, shoots were cut off and a new population of Col-0 plants (response population) was sown directly on top of the soil after which the experimental cycle was repeated⁵². For both the conditioning and response populations of plants, Hpa and gnoHpa sporulation was quantified as described above. Phyllosphere, rhizosphere and bulk soil samples were taken at the end of the growth period of the conditioning and response populations as described above. An overview of the experimental set-up described above is shown in Extended Data Fig. 5.

Statistics

The required sample replicate numbers sufficient to show statistically significant effects were estimated based on previous experience with similar bioassays. For Student's *t*-tests, the data distribution was assumed to be normal, but this was not formally tested. Individual data points have been included in the figures where possible.

Reporting summary

Further information on research design is available in the Nature Portfolio Reporting Summary linked to this article.

Data availability

The data that support the findings of this study and isolates are available from the corresponding author upon reasonable request. Moreover, the raw amplicon sequence data generated by this study are available at <https://www.ncbi.nlm.nih.gov/sra/PRJNA944652>; raw WGS data are available at <http://www.ncbi.nlm.nih.gov/bioproject/1011197>; genome assemblies generated in this study are available at <http://www.ncbi.nlm.nih.gov/bioproject/1011284>. Whenever possible, post-processing amplicon sequencing (ASV) count tables are also included together with the processing code at the Zenodo-archived GitHub page (<https://doi.org/10.5281/zenodo.8307753>). Source data are provided with this paper.

Code availability

The code used to analyse data and generate figures can be found at <https://doi.org/10.5281/zenodo.8307753>. No unpublished algorithms or methods were used.

References

- Kamoun, S. et al. The top 10 oomycete pathogens in molecular plant pathology. *Mol. Plant Pathol.* **16**, 413–434 (2015).
- Thines, M. & Choi, Y.-J. Evolution, diversity, and taxonomy of the *Peronosporaceae*, with focus on the genus *Peronospora*. *Phytopathology* **106**, 6–18 (2016).
- Ngou, B. P. M., Ding, P. & Jones, J. D. G. Thirty years of resistance: zig-zag through the plant immune system. *Plant Cell* **34**, 1447–1478 (2022).
- Parker, J. E. et al. Characterization of *eds1*, a mutation in *Arabidopsis* suppressing resistance to *Peronospora parasitica* specified by several different *RPP* genes. *Plant Cell* **8**, 2033–2046 (1996).
- Holub, E. B. in *The Downy Mildews—Genetics, Molecular Biology and Control* (eds Lebeda, A., Spencer-Phillips, P. T. N. & Cooke, B. N.) 91–109 (Springer, 2008).
- Vorholt, J. A. Microbial life in the phyllosphere. *Nat. Rev. Microbiol.* **10**, 828–840 (2012).
- Bakker, P. A. H. M., Berendsen, R. L., Doornbos, R. F., Wintermans, P. C. A. & Pieterse, C. M. J. The rhizosphere revisited: root microbiomics. *Front. Plant Sci.* **4**, 165 (2013).
- Rolfe, S. A., Griffiths, J. & Ton, J. Crying out for help with root exudates: adaptive mechanisms by which stressed plants assemble health-promoting soil microbiomes. *Curr. Opin. Microbiol.* **49**, 73–82 (2019).
- Liu, H., Brettell, L. E. & Singh, B. Linking the phyllosphere microbiome to plant health. *Trends Plant Sci.* **25**, 841–844 (2020).
- Pieterse, C. M. J. et al. Induced systemic resistance by beneficial microbes. *Annu. Rev. Phytopathol.* **52**, 347–375 (2014).
- Raaijmakers, J. M. & Mazzola, M. Diversity and natural functions of antibiotics produced by beneficial and plant pathogenic bacteria. *Annu. Rev. Phytopathol.* **50**, 403–424 (2012).
- Teixeira, P. J. P. L., Colaianni, N. R., Fitzpatrick, C. R. & Dangl, J. L. Beyond pathogens: microbiota interactions with the plant immune system. *Curr. Opin. Microbiol.* **49**, 7–17 (2019).
- Berendsen, R. L. et al. Disease-induced assemblage of a plant-beneficial bacterial consortium. *ISME J.* **12**, 1496–1507 (2018).
- Yuan, J. et al. Root exudates drive the soil-borne legacy of aboveground pathogen infection. *Microbiome* **6**, 156 (2018).
- Wen, T., Zhao, M., Yuan, J., Kowalchuk, G. A. & Shen, Q. Root exudates mediate plant defense against foliar pathogens by recruiting beneficial microbes. *Soil Ecol. Lett.* **3**, 42–51 (2021).
- Wang, Q. et al. Tea plants with gray blight have altered root exudates that recruit a beneficial rhizosphere microbiome to prime immunity against aboveground pathogen infection. *Front. Microbiol.* **12**, 3775 (2021).
- Friman, J. et al. Shoot and root insect herbivory change the plant rhizosphere microbiome and affects cabbage–insect interactions through plant–soil feedback. *New Phytol.* **232**, 2475–2490 (2021).
- Bakker, P. A. H. M., Pieterse, C. M. J., de Jonge, R. & Berendsen, R. L. The soil-borne legacy. *Cell* **172**, 1178–1180 (2018).
- Raaijmakers, J. M. & Mazzola, M. Soil immune responses. *Science* **352**, 1392–1393 (2016).
- Vismans, G. et al. Coumarin biosynthesis genes are required after foliar pathogen infection for the creation of a microbial soil-borne legacy that primes plants for SA-dependent defenses. *Sci. Rep.* **12**, 22473 (2022).
- Carrión, V. J. et al. Pathogen-induced activation of disease-suppressive functions in the endophytic root microbiome. *Science* **366**, 606–612 (2019).
- Schlatter, D., Kinkel, L., Thomashow, L., Weller, D. & Paulitz, T. Disease suppressive soils: new insights from the soil microbiome. *Phytopathology* **107**, 1284–1297 (2017).
- McDowell, J. M., Hoff, T., Anderson, R. G. & Deegan, D. in *Plant Immunity: Methods and Protocols* (ed McDowell, J. M.) 137–151 (Springer, 2011).
- Holub, E. B., Beynon, J. L. & Crute, I. R. Phenotypic and genotypic characterization of interactions between isolates of *Peronospora parasitica* and accessions of *Arabidopsis thaliana*. *Mol. Plant Microbe Interact.* **7**, 223–239 (1994).
- Parker, J. E. et al. Phenotypic characterization and molecular mapping of the *Arabidopsis thaliana* locus *RPP5*, determining disease resistance to *Peronospora parasitica*. *Plant J.* **4**, 821–831 (1993).

26. Love, M. I., Huber, W. & Anders, S. Moderated estimation of fold change and dispersion for RNA-seq data with DESeq2. *Genome Biol.* **15**, 550 (2014).
27. Lapin, D., Meyer, R. C., Takahashi, H., Bechtold, U. & Van den Ackerveken, G. Broad-spectrum resistance of *Arabidopsis* C24 to downy mildew is mediated by different combinations of isolate-specific loci. *New Phytol.* **196**, 1171–1181 (2012).
28. Nemri, A. et al. Genome-wide survey of *Arabidopsis* natural variation in downy mildew resistance using combined association and linkage mapping. *Proc. Natl Acad. Sci. USA* **107**, 10302–10307 (2010).
29. Olm, M. R. et al. InStrain enables population genomic analysis from metagenomic data and rigorous detection of identical microbial strains. *Nat. Biotechnol.* **39**, 727–736 (2021).
30. Baxter, L. et al. Signatures of adaptation to obligate biotrophy in the *Hyaloperonospora arabidopsidis* genome. *Science* **330**, 1549–1551 (2010).
31. Asai, S. et al. A downy mildew effector evades recognition by polymorphism of expression and subcellular localization. *Nat. Commun.* **9**, 5192 (2018).
32. Schaeffer, L., Pimentel, H., Bray, N., Melsted, P. & Pachter, L. Pseudoalignment for metagenomic read assignment. *Bioinformatics* **33**, 2082–2088 (2017).
33. Parker, J. E. et al. The *Arabidopsis* downy mildew resistance gene *RPP5* shares similarity to the toll and interleukin-1 receptors with N and L6. *Plant Cell* **9**, 879–894 (1997).
34. Lin, H. & Peddada, S. D. Analysis of compositions of microbiomes with bias correction. *Nat. Commun.* **11**, 3514 (2020).
35. Becking, L. G. M. B. *Geobiologie of inleiding tot de milieukunde* (W.P. Van Stockum & Zoon, 1934).
36. De Zutter, N. et al. Shifts in the rhizobiome during consecutive in planta enrichment for phosphate-solubilizing bacteria differentially affect maize P status. *Microb. Biotechnol.* **14**, 1594–1612 (2021).
37. Harbort, C. J. et al. Root-secreted coumarins and the microbiota interact to improve iron nutrition in *Arabidopsis*. *Cell Host Microbe* **28**, 825–837 (2020).
38. Santos-Medellín, C. et al. Prolonged drought imparts lasting compositional changes to the rice root microbiome. *Nat. Plants* **7**, 1065–1077 (2021).
39. Xu, L. et al. Genome-resolved metagenomics reveals role of iron metabolism in drought-induced rhizosphere microbiome dynamics. *Nat. Commun.* **12**, 3209 (2021).
40. Monohon, S. J., Manter, D. K. & Vivanco, J. M. Conditioned soils reveal plant-selected microbial communities that impact plant drought response. *Sci. Rep.* **11**, 21153 (2021).
41. Yuan, Y., Brunel, C., van Kleunen, M., Li, J. & Jin, Z. Salinity-induced changes in the rhizosphere microbiome improve salt tolerance of *Hibiscus hamabo*. *Plant Soil* **443**, 525–537 (2019).
42. Gao, M. et al. Disease-induced changes in plant microbiome assembly and functional adaptation. *Microbiome* **9**, 187 (2021).
43. Mendes, R. et al. Deciphering the rhizosphere microbiome for disease-suppressive bacteria. *Science* **332**, 1097–1100 (2011).
44. Weller, D. M., Raaijmakers, J. M., Gardener, B. B. M. & Thomashow, L. S. Microbial populations responsible for specific soil suppressiveness to plant pathogens. *Annu. Rev. Phytopathol.* **40**, 309–348 (2002).
45. Liu, X. et al. Phyllosphere microbiome induces host metabolic defence against rice false-smut disease. *Nat. Microbiol.* **8**, 1419–1433 (2023).
46. Bass, D., Stentiford, G. D., Wang, H.-C., Koskella, B. & Tyler, C. R. The pathobiome in animal and plant diseases. *Trends Ecol. Evol.* **34**, 996–1008 (2019).
47. Vayssier-Taussat, M. et al. Shifting the paradigm from pathogens to pathobiome: new concepts in the light of meta-omics. *Front. Cell. Infect. Microbiol.* **4**, 29 (2014).
48. Xu, S. et al. Fusarium fruiting body microbiome member *Pantoea agglomerans* inhibits fungal pathogenesis by targeting lipid rafts. *Nat. Microbiol.* **7**, 831–843 (2022).
49. Aarts, N. et al. Different requirements for *EDS1* and *NDR1* by disease resistance genes define at least two *R* gene-mediated signaling pathways in *Arabidopsis*. *Proc. Natl Acad. Sci. USA* **95**, 10306–10311 (1998).
50. Pieterse, C. M. J., Van Wees, S. C. M., Hoffland, E., Van Pelt, J. A. & Van Loon, L. C. Systemic resistance in *Arabidopsis* induced by biocontrol bacteria is independent of salicylic acid accumulation and pathogenesis-related gene expression. *Plant Cell* **8**, 1225–1237 (1996).
51. Lindsey III, B. E., Rivero, L., Calhoun, C. S., Grotewold, E. & Brkljacic, J. Standardized method for high-throughput sterilization of *Arabidopsis* seeds. *J. Vis. Exp.* **17**, 56587 (2017).
52. Vismans, G., Spooren, J., Pieterse, C. M. J., Bakker, P. A. H. M. & Berendsen, R. L. in *The Plant Microbiome: Methods and Protocols* Vol. 2232 (eds Carvalhais, L. C. & Dennis, P. G.) 209–218 (Springer, 2021).
53. Anderson, R. G. & McDowell, J. M. A PCR assay for the quantification of growth of the oomycete pathogen *Hyaloperonospora arabidopsidis* in *Arabidopsis thaliana*. *Mol. Plant Pathol.* **16**, 893–898 (2015).
54. de Muinck, E. J., Trosvik, P., Gilfillan, G. D., Hov, J. R. & Sundaram, A. Y. M. A novel ultra high-throughput 16S rRNA gene amplicon sequencing library preparation method for the Illumina HiSeq platform. *Microbiome* **5**, 68 (2017).
55. Lundberg, D. S., Yourstone, S., Mieczkowski, P., Jones, C. D. & Dangl, J. L. Practical innovations for high-throughput amplicon sequencing. *Nat. Methods* **10**, 999–1002 (2013).
56. Ihrmark, K. et al. New primers to amplify the fungal ITS2 region—evaluation by 454-sequencing of artificial and natural communities. *FEMS Microbiol. Ecol.* **82**, 666–677 (2012).
57. Agler, M. T., Mari, A., Dombrowski, N., Haquard, S. & Kemen, E. M. New insights in host-associated microbial diversity with broad and accurate taxonomic resolution. Preprint at *bioRxiv* <https://doi.org/10.1101/050005> (2016).
58. Bolyen, E. et al. Reproducible, interactive, scalable and extensible microbiome data science using QIIME 2. *Nat. Biotechnol.* **37**, 852–857 (2019).
59. Martin, M. Cutadapt removes adapter sequences from high-throughput sequencing reads. *EMBnet j.* **17**, 10–12 (2011).
60. Callahan, B. J. et al. DADA2: high-resolution sample inference from Illumina amplicon data. *Nat. Methods* **13**, 581–583 (2016).
61. King, E. O., Ward, M. K. & Raney, D. E. Two simple media for the demonstration of pyocyanin and fluorescein. *J. Lab. Clin. Med.* **44**, 301–307 (1954).
62. Bolger, A. M., Lohse, M. & Usadel, B. Trimmomatic: a flexible trimmer for Illumina sequence data. *Bioinformatics* **30**, 2114–2120 (2014).
63. Bankevich, A. et al. SPAdes: a new genome assembly algorithm and its applications to single-cell sequencing. *J. Comput. Biol.* **19**, 455–477 (2012).
64. Gurevich, A., Saveliev, V., Vyahhi, N. & Tesler, G. QUAST: quality assessment tool for genome assemblies. *Bioinformatics* **29**, 1072–1075 (2013).
65. Bray, N. L., Pimentel, H., Melsted, P. & Pachter, L. Near-optimal probabilistic RNA-seq quantification. *Nat. Biotechnol.* **34**, 525–527 (2016).
66. Murashige, T. & Skoog, F. A revised medium for rapid growth and bio assays with tobacco tissue cultures. *Physiol. Plant.* **15**, 473–497 (1962).

Acknowledgements

This study was sponsored by the TopSector Horticulture and Starting Materials (TKI grant number 1605-106), the Dutch Research Council (NWO) through the Gravitation programme MiCRop (grant number 024.004.014) and the XL programme 'Unwiring beneficial functions and regulatory networks in the plant endosphere' (grant number OCENW.GROOT.2019.063). The TKI project was carried out in collaboration with four industrial partners; DSM, Enza Zaden, Pop Vriend Seeds and RijkZwaan Breeding B.V. We thank J. Parker for providing Col-0 *RPP5* and Ler *rpp5* Arabidopsis seeds, P. Bakker and R. de Jonge for valuable input on experimental designs and bioinformatic approaches, and J. Elberse, D. Duijker, L. Pronk, C. Molina Ruiz, M. Alderkamp, X. Pan, L. Wagenaar and T. Tarrant for excellent technical assistance.

Author contributions

P.G., J.S., G.A., C.M.J.P. and R.L.B. designed the experiments and wrote the paper. R.L.B., G.A. and C.M.J.P. supervised the project and edited the paper. P.G. performed the experiments and data analysis shown in Figs. 1–4. D.L. performed the experiments in Cologne, Germany (Fig. 2). P.G. and N.E. performed the experiments shown in Fig. 5a,b. J.S. performed the experiments shown in Fig. 5c–e. P.G. and J.S. performed the experiments and data analysis shown in Fig. 6. K.C.M.B. and A.A. provided technical support during the conduct of the experiments and in the maintenance of Hpa and gnoHpa cultures.

Competing interests

The authors declare no competing interests.

Additional information

Extended data is available for this paper at <https://doi.org/10.1038/s41564-023-01502-y>.

Supplementary information The online version contains supplementary material available at <https://doi.org/10.1038/s41564-023-01502-y>.

Correspondence and requests for materials should be addressed to Roeland L. Berendsen.

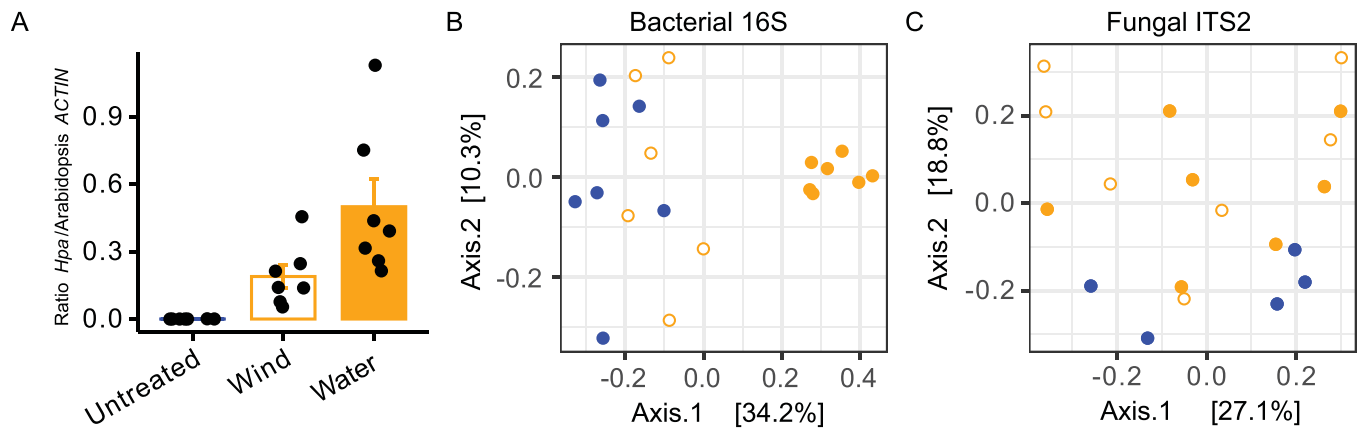
Peer review information *Nature Microbiology* thanks Yang Bai, Mengcen Wang and the other, anonymous, reviewer(s) for their contribution to the peer review of this work.

Reprints and permissions information is available at www.nature.com/reprints.

Publisher's note Springer Nature remains neutral with regard to jurisdictional claims in published maps and institutional affiliations.

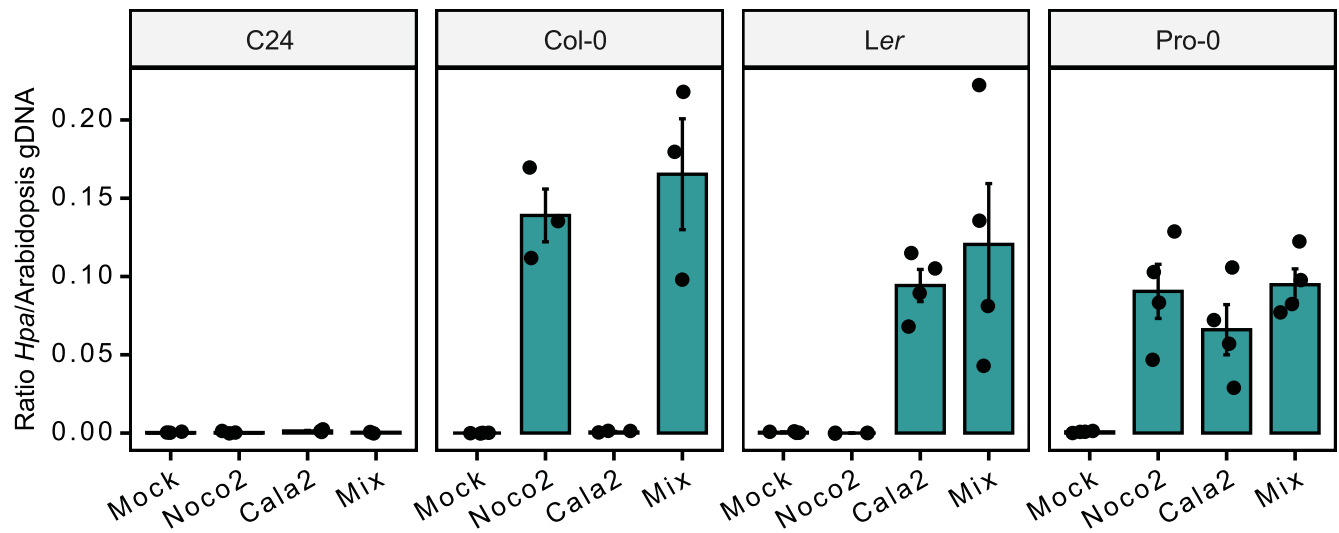
Springer Nature or its licensor (e.g. a society or other partner) holds exclusive rights to this article under a publishing agreement with the author(s) or other rightsholder(s); author self-archiving of the accepted manuscript version of this article is solely governed by the terms of such publishing agreement and applicable law.

© The Author(s), under exclusive licence to Springer Nature Limited 2023



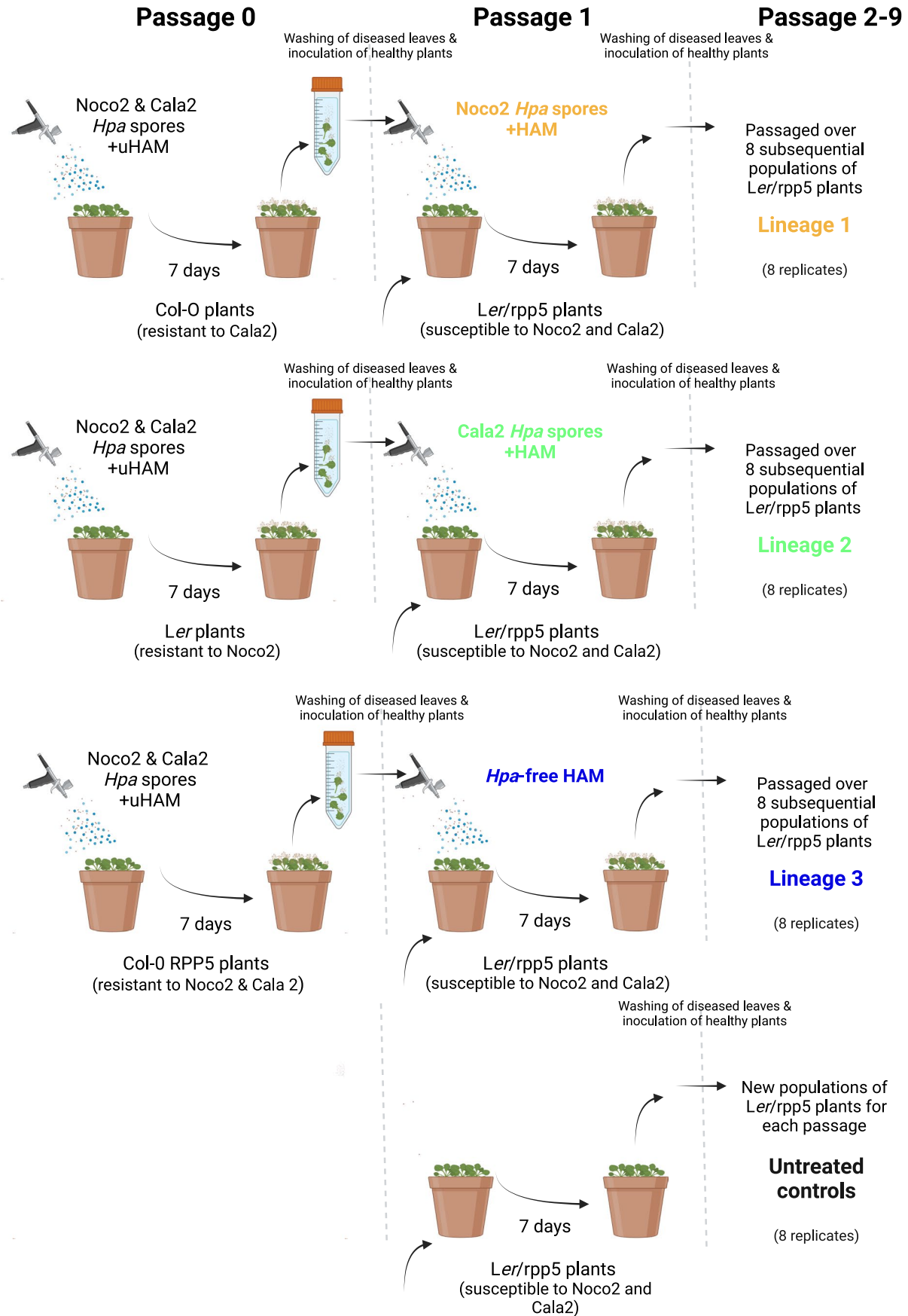
Extended Data Fig. 1 | Effect of water- and wind-transmitted *Hpa* infections on bacterial phyllosphere community structure. (a) Quantification of *Hpa* DNA relative to Arabidopsis DNA by qPCR for samples taken 7 days post-inoculation. Bars represent average *Hpa* abundance. Error bars show standard error. $N = 7$ biologically independent samples. PCoA ordination plot based on

Bray-Curtis dissimilarities of the (b) bacterial phyllosphere communities and (c) fungal phyllosphere communities of *Arabidopsis thaliana* Col-0 untreated control plants (blue symbols), or plants inoculated with *Hpa* spores via wind (orange stroke) or water (orange fill).



Extended Data Fig. 2 | Compatibility of *Noco2* and *Cala2* with susceptible and resistant *Arabidopsis* accessions. qPCR quantification of *Hpa* abundance in the susceptible and resistant *Hpa*-*Arabidopsis* interactions indicated, confirming that C24 is resistant to both *Noco2* and *Cala2*, that Col-0 is susceptible to *Noco2*, that *Ler* is susceptible to *Cala2*, and that Pro-0 is susceptible to both *Noco2* and *Cala2*. qPCR quantification was performed on total genomic DNA from

inoculated leaves that were also used for 16 S rDNA amplicon sequencing (Fig. 1). *Hpa* abundance was calculated as a ratio of the levels of *ACTIN* in *Hpa* and *Arabidopsis*. Bars represent average ratios, error bars represent standard error. $N = 4$ biologically independent samples, except for C24 mock-, *Noco2*-, and *Cala2*-treated ($N = 3$ biologically independent samples).

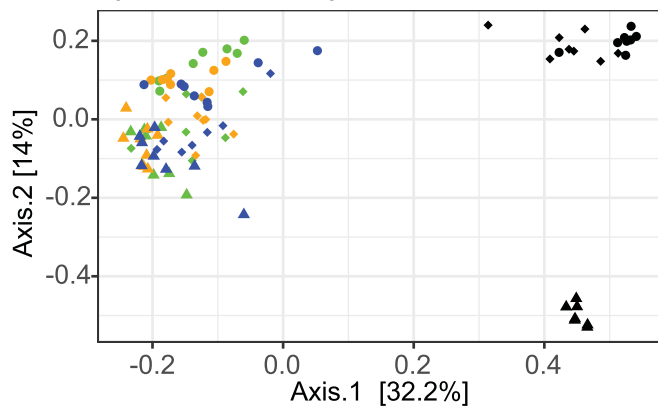
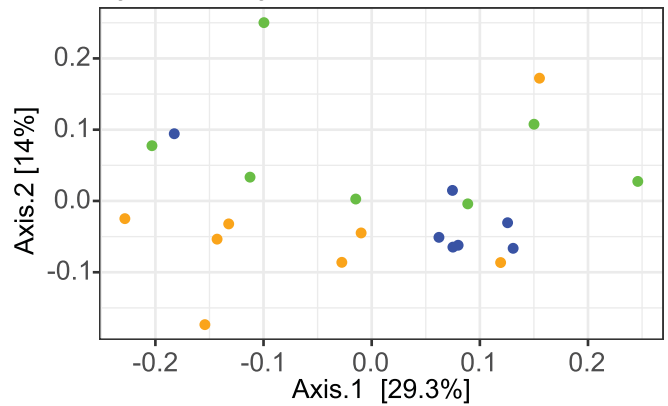
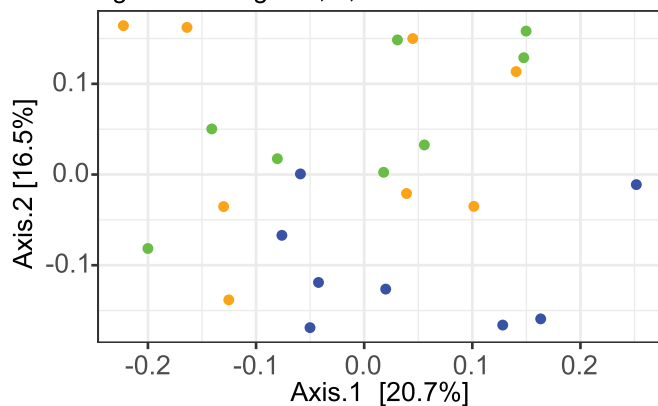
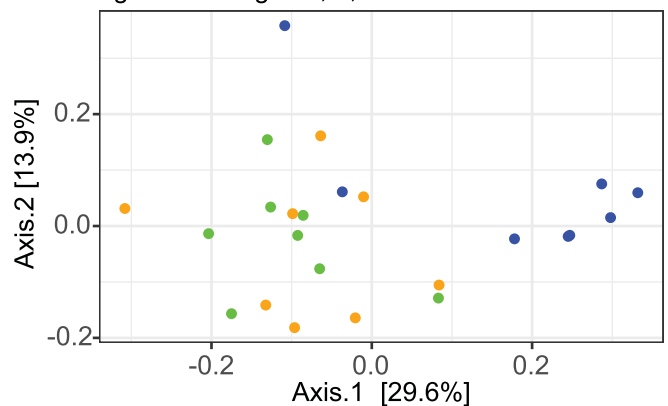


Extended Data Fig. 3 | See next page for caption.

Extended Data Fig. 3 | Schematic overview of the '9-passages experiment', which tests the effect of the removal of *Hpa* on its associated microbiome.

A uniform HAM (uHAM) containing a mix of Noco2 and Cala2 spore suspensions was spray-inoculated on different Arabidopsis genotypes to selectively remove Noco2 and/or Cala2 from the microbiome (HAM) that travels together with these *Hpa* isolates upon passaging to new host plants. One week post-inoculation, Col-0 (Lineage 1) and *Ler* plants (Lineage 2) sporulated with Noco2 and Cala2, respectively, and Col-0/*RPP5* transgenic plants (Lineage 3) did not sporulate. From each Arabidopsis genotype, a leaf wash-off was obtained, containing Noco2, Cala2, or no *Hpa*, and sprayed on eight pots containing small fields of *Ler/rpp5* mutant plants, which are susceptible to both Noco2 and Cala2.

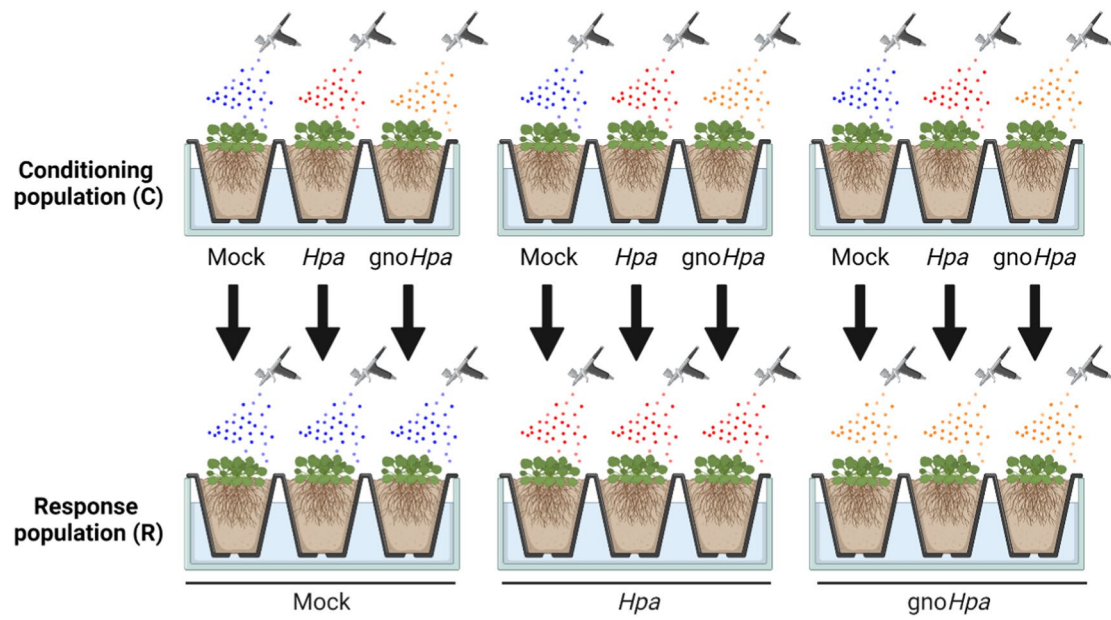
All pots were then placed in individual plastic containers, to prevent cross-contamination between pots. One week post-inoculation, the *Ler/rpp5* plants that were inoculated with Noco2 (Lineage 1) or Cala2 (Lineage 2), sporulated, while the *Ler/rpp5* plants that were inoculated with the leaf wash-off without *Hpa* spores (Lineage 3) did not display disease symptoms. From each individual pot, the leaf wash-off was sprayed on a new pot containing *Ler/rpp5* plants, thereby propagating eight separate phyllosphere microbiomes or *Hpa* cultures per lineage. This process was maintained for nine consecutive weeks, allowing eight separate lineages of Noco2, Cala2, or the uHAM without *Hpa* to develop independently. Eight untreated control pots with *Ler/rpp5* plants were included for all planting cycles.

A Passages 1, 5, 9 - Lineages 1, 2, 3, and untreated**B** Passage 1 - Lineages 1, 2, 3**C** Passage 5 - Lineages 1, 2, 3**D** Passage 9 - Lineages 1, 2, 3

● Untreated ● Lineage 1 (Noco2 spores) ● Lineage 2 (Cala2 spores) ● Lineage 3 (no spores)

Extended Data Fig. 4 | The *Hpa*-culture bacterial community is largely unaffected by removal of *Hpa*, but nonetheless there are community shifts in the absence of *Hpa*. PcoA plots based on Bray-Curtis dissimilarities of (a) all samples from Lineages 1–3 and untreated plants of passages 1 (circles), passage 5 (triangles) and passage 9 (diamonds); and of all inoculated samples of Lineage

1–3 from (b) passage 1, (c) passage 5, and (d) passage 9. Plants were left untreated (black symbols) or were inoculated with leaf wash-offs from Lineage 1 containing Noco2 (orange symbols), from Lineage 2 containing Cala2 (green symbols), or from Lineage 3 which remained *Hpa* free (blue symbols).



Extended Data Fig. 5 | Setup of soil-borne legacy experiments. A conditioning population of two-week-old *Arabidopsis thaliana* Col- seedlings was inoculated with mock, *Hpa* Noco2 or *gnoHpa* Noco2. After one week of infection, shoots

were cut-off and a response population of plants was directly sown on the conditioned soil and again mock- *Hpa*- or *gnoHpa*-inoculated. Figure created with [BioRender.com](https://www.biorender.com).

Reporting Summary

Nature Portfolio wishes to improve the reproducibility of the work that we publish. This form provides structure for consistency and transparency in reporting. For further information on Nature Portfolio policies, see our [Editorial Policies](#) and the [Editorial Policy Checklist](#).

Statistics

For all statistical analyses, confirm that the following items are present in the figure legend, table legend, main text, or Methods section.

- | n/a | Confirmed |
|-------------------------------------|--|
| <input type="checkbox"/> | <input checked="" type="checkbox"/> The exact sample size (n) for each experimental group/condition, given as a discrete number and unit of measurement |
| <input type="checkbox"/> | <input checked="" type="checkbox"/> A statement on whether measurements were taken from distinct samples or whether the same sample was measured repeatedly |
| <input type="checkbox"/> | <input checked="" type="checkbox"/> The statistical test(s) used AND whether they are one- or two-sided
<i>Only common tests should be described solely by name; describe more complex techniques in the Methods section.</i> |
| <input type="checkbox"/> | <input checked="" type="checkbox"/> A description of all covariates tested |
| <input type="checkbox"/> | <input checked="" type="checkbox"/> A description of any assumptions or corrections, such as tests of normality and adjustment for multiple comparisons |
| <input type="checkbox"/> | <input checked="" type="checkbox"/> A full description of the statistical parameters including central tendency (e.g. means) or other basic estimates (e.g. regression coefficient) AND variation (e.g. standard deviation) or associated estimates of uncertainty (e.g. confidence intervals) |
| <input type="checkbox"/> | <input checked="" type="checkbox"/> For null hypothesis testing, the test statistic (e.g. F , t , r) with confidence intervals, effect sizes, degrees of freedom and P value noted
<i>Give P values as exact values whenever suitable.</i> |
| <input checked="" type="checkbox"/> | <input type="checkbox"/> For Bayesian analysis, information on the choice of priors and Markov chain Monte Carlo settings |
| <input checked="" type="checkbox"/> | <input type="checkbox"/> For hierarchical and complex designs, identification of the appropriate level for tests and full reporting of outcomes |
| <input type="checkbox"/> | <input checked="" type="checkbox"/> Estimates of effect sizes (e.g. Cohen's d , Pearson's r), indicating how they were calculated |

Our web collection on [statistics for biologists](#) contains articles on many of the points above.

Software and code

Policy information about [availability of computer code](#)

Data collection The code used to analyze data and generate figures can be found at DOI: 10.5281/zenodo.8307753. No unpublished algorithms or methods were used.

Data analysis Amplicon sequencing data analyses: Qiime2 (version 2019.7); R (version 4.0.3). R packages: vegan (version 2.5.7), phyloseq (version 1.34.0), pairwiseAdonis (version 0.0.1), DESeq2 (version 1.30.1). WGS data processing: Trimmomatic (version 0.39), Spades (version 3.11.1)

For manuscripts utilizing custom algorithms or software that are central to the research but not yet described in published literature, software must be made available to editors and reviewers. We strongly encourage code deposition in a community repository (e.g. GitHub). See the Nature Portfolio [guidelines for submitting code & software](#) for further information.

Data

Policy information about [availability of data](#)

All manuscripts must include a [data availability statement](#). This statement should provide the following information, where applicable:

- Accession codes, unique identifiers, or web links for publicly available datasets
- A description of any restrictions on data availability
- For clinical datasets or third party data, please ensure that the statement adheres to our [policy](#)

The data that support the findings of this study and isolates are available from the corresponding author upon reasonable request. Moreover, the raw amplicon sequence data generated of this study are available under PRJNA944652; raw WGS sequencing data is available under PRJNA1011197; genome assemblies

generated in this study are available under PRJNA1011284.

Whenever possible, post-processing amplicon sequencing (ASV) count tables are also included together with processing code at DOI: 10.5281/zenodo.8307753. Taxonomic assignment of 16S ASVs was based on the SILVA database (QIIME compatible 138 release, 99% clustering identity, 7-level RDP-compatible consensus taxonomies). Fungal ITS amplicons were taxonomically assigned based on the UNITE fungal database (QIIME release, version 7.2, 99% similarity clustering, 7-level taxonomies). Sequence data described in the publication by Baxter et al. 30, that was obtained from Emoy2 spores collected in water (similar to the Hpa inocula used in the present study), were obtained in fasta format from the NCBI TRACE archive using query 'species_code='HYALOPERONOSPORA PARASITICA'. Sequence data described in the publication by Asai et al. 31 were obtained from the European Nucleotide Archive under project number PRJEB22892.

Research involving human participants, their data, or biological material

Policy information about studies with [human participants or human data](#). See also policy information about [sex, gender \(identity/presentation\), and sexual orientation](#) and [race, ethnicity and racism](#).

Reporting on sex and gender

Use the terms sex (biological attribute) and gender (shaped by social and cultural circumstances) carefully in order to avoid confusing both terms. Indicate if findings apply to only one sex or gender; describe whether sex and gender were considered in study design; whether sex and/or gender was determined based on self-reporting or assigned and methods used. Provide in the source data disaggregated sex and gender data, where this information has been collected, and if consent has been obtained for sharing of individual-level data; provide overall numbers in this Reporting Summary. Please state if this information has not been collected. Report sex- and gender-based analyses where performed, justify reasons for lack of sex- and gender-based analysis.

Reporting on race, ethnicity, or other socially relevant groupings

Please specify the socially constructed or socially relevant categorization variable(s) used in your manuscript and explain why they were used. Please note that such variables should not be used as proxies for other socially constructed/relevant variables (for example, race or ethnicity should not be used as a proxy for socioeconomic status). Provide clear definitions of the relevant terms used, how they were provided (by the participants/respondents, the researchers, or third parties), and the method(s) used to classify people into the different categories (e.g. self-report, census or administrative data, social media data, etc.) Please provide details about how you controlled for confounding variables in your analyses.

Population characteristics

Describe the covariate-relevant population characteristics of the human research participants (e.g. age, genotypic information, past and current diagnosis and treatment categories). If you filled out the behavioural & social sciences study design questions and have nothing to add here, write "See above."

Recruitment

Describe how participants were recruited. Outline any potential self-selection bias or other biases that may be present and how these are likely to impact results.

Ethics oversight

Identify the organization(s) that approved the study protocol.

Note that full information on the approval of the study protocol must also be provided in the manuscript.

Field-specific reporting

Please select the one below that is the best fit for your research. If you are not sure, read the appropriate sections before making your selection.

Life sciences Behavioural & social sciences Ecological, evolutionary & environmental sciences

For a reference copy of the document with all sections, see [nature.com/documents/nr-reporting-summary-flat.pdf](https://www.nature.com/documents/nr-reporting-summary-flat.pdf)

Life sciences study design

All studies must disclose on these points even when the disclosure is negative.

Sample size

Sample sizes were chosen based on previous experiences with variance in bioassays (> 8 replicates needed). For sequencing data, the number of replicates is a balance, based on previous experiences, between enough replicates to get statistical power, and cost management.

Data exclusions

In the sequencing data underlying Figure 6, two rhizosphere samples named R-G-GI-4 and R-G-GI-8 were excluded since they were sampled as 'rhizosphere', but in PCoA analysis clearly clustered towards bulk samples. Based on this observation deemed these samples as not representative for rhizosphere, which is the sample-type that we intended to study. Other than this no data was excluded.

Replication

All bioassays were performed at least 2-times with similar results. All sequencing based experiments were performed once as the budgetary and time investments for the sequencing and analysis were already considerable.

Randomization

For every experiment, all pots/ treatments were randomized within trays and throughout the growth chambers. Also during sampling, the processing of samples, replicate samples were handled in randomized order as much as possible.

Blinding

Experiments were not performed blind. Dependent variable measurements (e.g. ASV counts as determined by sequencing) were not subjective and blinding would have unnecessarily complicated the experiments.

Reporting for specific materials, systems and methods

We require information from authors about some types of materials, experimental systems and methods used in many studies. Here, indicate whether each material, system or method listed is relevant to your study. If you are not sure if a list item applies to your research, read the appropriate section before selecting a response.

Materials & experimental systems

- | n/a | Included in the study |
|-------------------------------------|--|
| <input checked="" type="checkbox"/> | <input type="checkbox"/> Antibodies |
| <input checked="" type="checkbox"/> | <input type="checkbox"/> Eukaryotic cell lines |
| <input checked="" type="checkbox"/> | <input type="checkbox"/> Palaeontology and archaeology |
| <input checked="" type="checkbox"/> | <input type="checkbox"/> Animals and other organisms |
| <input checked="" type="checkbox"/> | <input type="checkbox"/> Clinical data |
| <input checked="" type="checkbox"/> | <input type="checkbox"/> Dual use research of concern |
| <input type="checkbox"/> | <input checked="" type="checkbox"/> Plants |

Methods

- | n/a | Included in the study |
|-------------------------------------|---|
| <input checked="" type="checkbox"/> | <input type="checkbox"/> ChIP-seq |
| <input checked="" type="checkbox"/> | <input type="checkbox"/> Flow cytometry |
| <input checked="" type="checkbox"/> | <input type="checkbox"/> MRI-based neuroimaging |